FORSCHUNGSZENTRUM JÜLICH GmbH KFA

Institut für Plasmaphysik
Association EURATOM-KFA

One dimensional model of a tokamak edge plasma under conditions of strong impurity radiation

M.Z. Tokar'

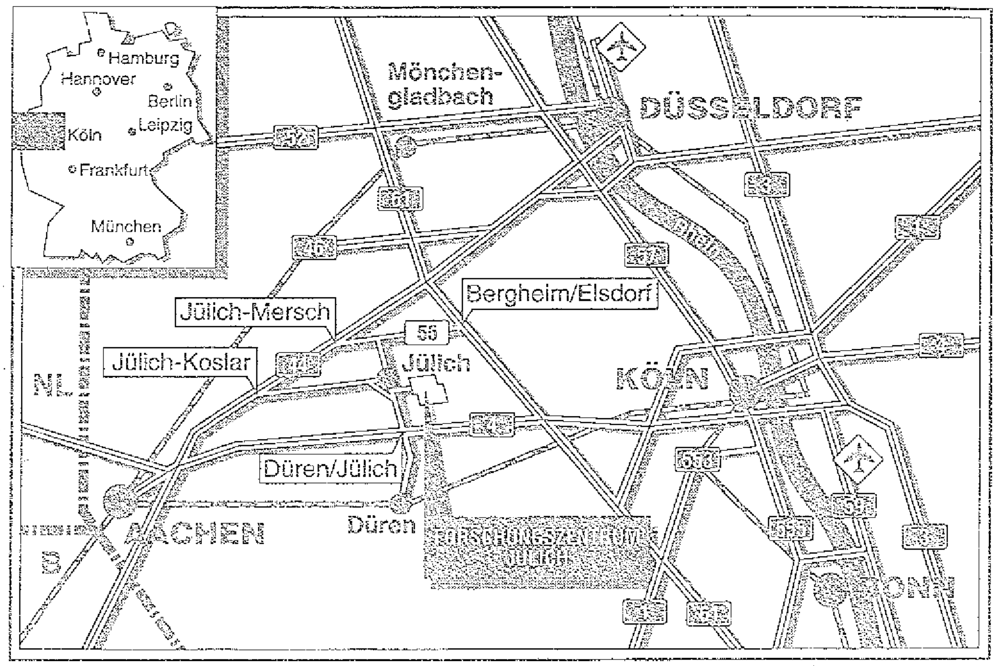

Berichte des Forschungszentrums Jülich ; 2588
ISSN 0366-0885
Institut für Plasmaphysik Jül-2588
Association EURATOM-KFA

Zu beziehen durch: Forschungszentrum Jülich GmbH · Zentralbibliothek
Postfach 1913 · D-5170 Jülich · Bundesrepublik Deutschland
Telefon: 02461/61-6102 · Telefax: 02461/61-6103 · Telex: 833556-70 kfa d

One dimensional model of a tokamak edge plasma under conditions of strong impurity radiation

M.Z. Tokar'

ABSTRACT

The edge plasma in tokamaks (within the last closed magnetic surface touching the limiter) is studied theoretically under conditions when the radiation from light impurities makes a strong contribution to its thermal balance. Simple appoximative formulas are proposed for the dependences of cooling rates of impurity ions on the electron temperature. A theory is developed for the so-called radiative potential equal the energy losses by electrons on the ionization and excitation of an impurity particle entering the discharge. The conditions of the onset of the states with "detached plasma" are explained for discharges with ohmic heating. The discharges with auxiliary heating and neon puffing are studied. The theory results are compared in detail with the experimental data from TEXTOR.

TABLE OF CONTENTS

1. INTRODUCTION

The problem of hot plasma interaction with the material walls is one of the burning questions, solution of which is essential for the creation of a viable thermonuclear reactor. The estimates, done under the ITER project[1], show that with a temperature of the edge plasma of some tens of electron volts, the erosion of the divertor plates will come to more than 10 cm in a year of continuous operation. This is absolutely unacceptable from the technical point of view.

The temperature of the plasma in a contact with the wall elements and the heat loads on them can be reduced by an increase of impurity radiation from the discharge[2]. However, the source of radiation should be localized in the peripheral region and impurities should not contribute significantly to the energy balance of the central plasma and hinder its heating up to thermonuclear temperatures. The light impurities - from boron to neon - satisfy these requirements since they are ionized up to the helium-like states in a relatively thin layer at the discharge edge. The energy losses by electrons on the excitation of low ionized impurity particles exceed the bremsstrahlung losses due to the presence of their nuclei in the discharge centre by $\sim 10^3$ times[3]. For heavy metallic impurities like iron this ratio is much lower and their influence is much stronger on the plasma core than on its periphery.

In the discharges with ohmic heating the onset of the states with strong radiation from impurities from the edge, which was called "detachment", occurs spontaneously when the density increases up to a certain critical level[2]. This results from the carbon particle presence in the plasma due to erosion of the device walls. With the presence of oxygen the critical density decreases strongly. In the state with "detached plasma" the source of radiation is localized in a toroidally-symmetric layer within the last closed magnetic surface(LCMS). With a further increase of the density the radius of the radiating layer decreases and when it reaches the rational magnetic surface with the safety factor equal to two a disruption takes place[4].

In the discharges with strong auxiliary heating, intrinsic impurities, released due to the wall erosion, do not radiate enough to influence substantially heat balance of the edge plasma*. To achieve this a puffing of some gaseous impurities, for example neon, is usually used.

The TEXTOR experiments[7] have shown, that more than 95% of the power, transported to the edge, can be radiated by neon without detachment, so the source of radiation stays in the vicinity of the LCMS. It is remarkable that with the increase of radiation up to this level the helium exhaust from the discharge does not deteriorate[8].

Importance of the cited results requires a construction of adequate theoretical models for the description of the tokamak plasma transition and evolution into the states with strong impurity radiation from the edge. Usually such a modelling is restricted either by a qualitative zero-dimensional consideration or by calculation of radiative losses for some typical profiles of the plasma parameters. The review of such models is given in Ref.[9]. At the same time the experiments show[2] a qualitative changing of the profiles with the increase of radiation. Thus the self-consistent description of the background plasma and impurities is necessary. The present paper summarizes the results of the author's theoretical activity in this direction during the past year.

The structure of the paper is the following. In Section 2 we discuss the model used to describe physical processes in the tokamak peripheral region, the basic assumptions and equations are formulated, the data base for the constants of elementary process is given. In Section 3 discharges with ohmic heating are discussed under assumption of the neo-Alcator scaling for the transport coefficients across the magnetic field; a theory is developed for the "radiative potential" - the total radiative losses by electrons on the ionization and excitation of an impurity particle entering the discharge. Section 4 is devoted to the modelling of discharges with a strong auxiliary heating and neon puffing. The main results of the paper are summarized in Section 5. The adequacy of the assumptions in the model for the particular experimental conditions is discussed in a supplement.

°We do not discuss some special modes of the plasma-surface interaction like "hot spots"[5,6] here.

2. THE MODEL

The present one-dimensional model is intended for the calculations of parameters averaged over the magnetic surfaces (under the conditions when such an averaging is applicable) and any conclusion can not be done on its basis about their local values.

2.1. Main assumption

a. We consider the peripheral region of a tokamak with a toroidal limiter(Fig.1) - the region inside the LCMS, where the neutrals of hydrogen isotopes and the ions of light impurities up to the lithium-like states inclusive are localized. Since the width of this region is small in comparison with the minor radius of the LCMS, a plane geometry is applicable for its description.

b. The deuterium atoms, coming into the plasma from the limiter, have two characteristic values of kinetic energy : the slow atoms, which appear as a result of the dissociation of molecules, have an energy of the Franck-Condon transition of the order of 1 eV; the atoms, appearing by the ion reflection and having an energy of the order of the plasma temperature at the LCMS. The neutral influx is determined by the condition of the total recycling of particles on the limiter. The atoms, which appear in the plasma during the charge-exchange of the primary atoms with ions, are described in the diffusive approximation. This approximation is applicable strictly speaking when the path length of atoms before charge-exchange is much shorter than that before ionization and than the scale of the ion temperature change.

c. The influx of intrinsic impurity atoms is connected with the deuteron flux onto the limiter through the erosion coefficient; in the case of recycling impurities like neon their concentration in the plasma is prescribed. The velocities of impurity atoms are determined by the physics of their release: it is physical and chemical sputtering in the case of carbon and oxygen[10]; the energy of neon neutrals depends on the conditions of ion reflection from the limiter.

d. The scrape-off layer(SOL) of the limiter is transparent for the neutrals of deuterium and impurities i.e. the particle and energy sources and sinks are negligible in the SOL plasma. This means that the charged particle temperatures do not change strongly in the SOL.

e. Since the density of the heat flux across the magnetic surfaces is constant, the Shafranov shift is ignored and assume, that the equilibrium system of a machine does not support asymmetric states like MARFE as it is done in TEXTOR [11]. Strong changes of the plasma parameters along B in the peripheral region, due to recycling localizing on the limiter, do not occur. Therefore the transport equations can be averaged over the magnetic surfaces. As it was shown recently[33], in the case of impurities such an averaging results in neoclassical-like drift fluxes across the magnetic surfaces. We do not take these fluxes into account assuming that the anomalous diffusion prevails.

f. The charged particle diffusivities across the magnetic surfaces are the same for all species - electrons, deuterons and impurity ions. The temperatures of ions and electrons are equal each other. Energy sources within the peripheral region are not essential and heat is transported here from the discharge core by heat conduction.

g. The radiative, dielectronic, three-body recombinations of impurity and its charge-exchange rate with deuterium neutrals, are negligible in comparison with the ionization by electrons and diffusion. The effect of the plasma dilution by impurities is not taken into account i.e. the densities of electrons and deuterons are assumed equal.

The adequacy of these assumptions for the experimental conditions in question is discussed in the Supplement.

2.2. The equations of particle and heat balances.

In the framework of the above mentioned assumptions the transport equations for neutral and charged particles and energy in the peripheral plasma, averaged over the magnetic surfaces, have the following form:

the continuity equations

deuterium atoms

$$\frac{d}{dx} (v_a^{1,2} n_a^{1,2}) = - (k_i^a + k_c) n n_a^{1,2} \tag{1a}$$

$$\frac{d}{dx} (- D_a \frac{dn_a^*}{dx}) = - k_i^a n n_a^* + k_c n (n_a^1 + n_a^2) \tag{1b}$$

impurity atoms

$$\frac{d}{dx} (v_0 n_0) = - k_i^0 n n_0 \tag{2}$$

deuterons

$$- \frac{d\Gamma_\perp}{dx} = k_i^a n (n_a^* + n_a^1 + n_a^2) \tag{3}$$

impurity ions

$$- \frac{d\Gamma_\perp^z}{dx} = k_i^{z-1} n n_{z-1} - k_i^z n n_z \tag{4}$$

the plasma heat balance

$$- \frac{dq_\perp}{dx} = - k_i^a n (n_a^* + n_a^1 + n_a^2) E_i - \sum_{1 \le z \le z_{Li}} n n_z L_z \tag{5}$$

Here x is the distance from the LCMS, $n_a^{1,2,*}$ are the densities of Franck-Condon, reflected and charge-exchanged deuterium atoms, n_0 is the density of impurity atoms, $v_a^{1,2}$, v_0 are the velocities of neutral particles; n, T are the plasma density and temperature, n_z is the density of the impurity ions with the charge z, z_{Li} is the charge of the lithium-like ions; $\Gamma_\perp = D_\perp dn/dx$, $\Gamma_\perp^z = D_\perp dn_z/dx$, $q_\perp = \kappa_\perp dT/dx + \alpha\Gamma_\perp T$ are the densities of the particle and heat fluxes in the direction to the LCMS, $D_\perp, \kappa_\perp$ are the diffusivity and heat conductivity across the magnetic surfaces, E_a, L_z are the energy losses by electrons on the ionization and excitation of deuterium atoms and impurity ions, respectively.

The diffusivity of deuterium atoms in the plasma due to their charge-exchange is given by the formula[12,13]

$$D_a = \frac{2\,T}{m_i\,(\,k_i^a + k_c\,)\,n}$$

where k_c is the constant of charge-exchange.

The formulas used for heat conductivity of the plasma and the charged particle diffusivity are given in the appropriate sections.

2.3. The boundary conditions.

The boundary conditions of the system (1)-(5) are posed at the LCMS ($x=0$) and at the conventional border between the peripheral region and the central part of the discharge($x=x_0$); the latter is determined by the condition that with $x \geq x_0$ the atoms of deuterium and impurity, the impurity ions with $z \leq z_{Li}$ are practically absent:

$x=0$:

the recycling of deuterium neutrals

$$n_a^1\, v_a^1 = (\Gamma_\perp + n_a^* v_i)\,(1-R_N)\;,\quad n_a^2\, v_a^2 = (\Gamma_\perp + n_a^* v_i)\,R_N\;,\quad D_a\,\frac{dn_a^*}{dx} = n_a^*\, v_i \tag{6a}$$

impurity atom flux

$$n_0\, v_0 = S_I\, \Gamma_\perp \tag{6b}$$

the continuity of particle and heat fluxes

$$\Gamma_\perp = n\, V_*\;,\quad \Gamma_\perp^z = n_z\, V_*^z \tag{7b}$$

$$q_\perp = \gamma_s\, \Gamma_\perp T \tag{7b}$$

where R_N is the reflection coefficient of particles, V_*, V_*^z, γ_s are determined by the transport of particles and heat in the SOL; when volumetric sources and sinks of particles and heat are negligible in the SOL[13] $V_* \approx V_*^z \approx (D_\perp^s V_s/L_s)^{1/2}$ ($D_\perp^s$ is the transverse diffusivity, L_s is the connection length in the SOL, $V_s=(2T/m_i)^{1/2}$) and $\gamma_s \approx 7$-10 is the heat transfer factor from the plasma to an isolated surface; S_I is the erosion coefficient and according to Ref.[10] $S_I \approx 0.03$ in the case of carbon, for neon S_I is determined by neon concentration in the discharge;

$x=x_0$:

$$n_a^{1,2,*} = n_{0 \leq z \leq z_{Li}} = 0 \tag{8}$$

$$n = n_b\;,\quad q_\perp = q_0 \tag{9}$$

The plasma density at $x=x_0$, n_b, is determined by the mean density in the discharge $\langle n \rangle$ and if the profile of n is not strongly peaked $n_b \approx \langle n \rangle$, q_0 is given by the total power, launched into the plasma.

2.4. The constants of elementary processes.

The following simple approximative formula is used for the temperature dependences of the ionization constants:

$$k_i = \frac{A_i \sqrt{T_e} \exp(-I/T_e)}{1 + C_i T_e} \tag{10}$$

The magnitudes of the ionization potentials I and constants A_i, C_i for different atoms were found using the data of Ref.[14,15] and are presented in the Table:

Table 1

species	I,eV	$A_i, 10^{-9} cm^3 s^{-1} eV^{-1/2}$	C_i, 10^{-3} eV^{-1}
H^0	13.6	7.3	10
He^0	24.6	3.6	4.6
He^+	54.4	0.32	3.1
C^0	11.3	26.8	10
C^+	24.4	5.9	6.3
C^{2+}	48	1.34	4.1
C^{3+}	64.5	0.27	1.73
O^0	13.6	11	2.86
O^+	35.1	3.8	2.65
O^{2+}	54.9	2	2.73
O^{3+}	77.4	0.68	1.85
O^{4+}	104	0.26	1.78
O^{5+}	138.1	0.072	0.66
Ne^0	21.6	5.1	2.38
Ne^+	41.1	2.72	1.81
Ne^{2+}	63.5	1.45	1.15
Ne^{3+}	92.5	0.77	1.45

Ne^{4+}	126.2	0.33	1.45
Ne^{5+}	157.9	0.19	1.26
Ne^{6+}	207.5	0.067	0.89
Ne^{7+}	239.1	0.024	0.46

The cooling rates of impurity ions L_z are calculated under assumption of coronal equilibrium for excited states of the ions with given z. This means that the collisional excitation by electrons is equilibrated by the radiative de-excitation:

$$L_z = \sum_{i,j} (k_{ex}^{i,j} E_{i,j} + k_i^z I_z) \qquad (11)$$

where $k_{ex}^{i,j}$ is the constant of excitation and $E_{i,j}$ is the energy of the transition between the levels with quantum numbers i and j.

In Ref.[16] the T_e-dependences of $k_{ex}^{i,j}$ are given for carbon and oxygen ions. Using them we have approximated $L_z(T_e)$ as follows:

$$L_z = \frac{A_e \sqrt{T_e}\, \exp(-E/T_e)}{1 + B_e \sqrt{T_e} + C_e T_e} \qquad (12)$$

The "activation" energies E and coefficients A_e, B_e, C_e are presented in the Table 2; the numbers of the transitions taking into account are also given there

Table 2

species	E,eV	A_e,10^{-7} $eV^{½}cm^3c^{-1}$	B_e,$eV^{-½}$	C_e,$10^{-3}eV^{-1}$	number of transitions
C^+	7.76	5.6	0.21	14.3	7
C^{2+}	7.59	7.27	0.265	23	11
C^{3+}	5.48	7.54	0.483	56.5	4
O^+	6.23	1.04	0	25	4
O^{2+}	7.94	1.59	0	28.2	8
O^{3+}	7.61	1.41	0	9.5	6
O^{4+}	9.7	2.7	0	14.3	11
O^{5+}	4.13	1.05	0.2	13.4	4

The data base for the excitation constants of neon ions isn't so comprehensive as for carbon and oxygen. In the literature[17-19] we only found information about some transitions and therefore used the following procedure for determination of $L_z(T_e)$. For a transition in neon ions with charge z, for which $k_{ex}{}^{i,j}$, $E_{i,j}$ are known, we calculated the ratio ω of $k_{ex}{}^{i,j}E_{i,j}$ to the cooling rate of the corresponding transition in the isoelectronic ion of oxygen with charge z-2. These ratios weakly depend on T_e. For example for the transition $2s^2 2p\,^2P_{3/2} \rightarrow 2s^2 p^{2\,2}P_{3/2}$ in ions O^{3+} and Ne^{5+} ω is practically constant with $T_e > 20$ eV and is close to 0.55. For the transition $2s^{2\,1}S \rightarrow 2s^2 p\,^1P$ in ions O^{4+} and Ne^{6+} $\omega \approx 0.7$ with $T_e > 30$ eV. We assume, that the same relation is correct for others transitions in isoelectronic ions, so L_z for neon ions can be calculated multiplying L_{z-2} for oxygen on ω.

Fig.2 and Fig.3 show how our approximative formulas for $k_{ex}{}^{i,j}$ and $L_z(T_e)$ agree with the data of Ref.[14-16]. Energy losses by electrons on the ionization and excitation of deuterium atoms depend on n and T_e weakly relatively with $T_e > 5$ eV and according to Ref.[20] we take $E_i = 25$eV.

3. OHMIC DISCHARGES

3.1. The transport equations in dimensionless variables.

In the discharges with ohmic heating of the plasma the transverse diffusivity and heat conductivity are described by the neo-Alcator scaling:

$$D_\perp = \frac{A_D\,(T_e\,)}{n}\,, \quad \kappa_\perp = \frac{A_D}{\varepsilon_D} \tag{13}$$

where A_D, ε_D do not depend on the plasma density.

In such a case Eqs.(1)-(6) can be reduced to a more simple form with introduction of the following dimensionless variables

$$u = \sigma_0 \int_0^x n\,dx\,, \quad \eta_a^{1,2,*} = \frac{n_a^{1,2,*}\,V_s^s}{\Gamma_s}\,, \quad \eta_z = \frac{n_z}{n_0(0)}\,, \quad \eta = \frac{A_D(T_s)\,\sigma_0\,n}{\Gamma_s}$$

where

$$\sigma_0 = 10^{-14}\,cm^2\,, \quad T_s = T(0)\,, \quad \Gamma_s = \Gamma_\perp(0)\,, \quad V_s^s = V_s(0)$$

As a result instead of (1)-(6) one has the following system of equations:

$$\frac{d\eta_a^{1,2}}{du} = -\,\lambda_a^{1,2}\,\eta_a^{1,2}\,, \quad \frac{d^2\eta_a^*}{du^2} + w_a^*\,\frac{d\eta_a^*}{du} = (\lambda_a^*)^2\,\eta_a^* \tag{14a}$$

$$\frac{d\eta_0}{du} = -\,\lambda_{00}\,\eta_0 \tag{14b}$$

$$\lambda_p \frac{d\eta}{du} = \beta_1 \eta_a^1 + \beta_2 \eta_a^2 - \beta_* \frac{d\eta_a^*}{du} \tag{14c}$$

$$\lambda_p \frac{d^2\eta_z}{du^2} = \lambda_z^2 \eta_z - \lambda_{z-1}^2 \eta_{z-1} \tag{14d}$$

$$\frac{d}{du}\left(\lambda_p\left(\frac{\eta}{\varepsilon_D}\frac{dT}{du} + (\alpha T+E_a)\frac{d\eta}{du}\right)\right) = \frac{S_I}{\sigma_0 v_0} \sum_{1\leq z\leq z_U} L_z(T(u))\,\eta_z \tag{14e}$$

Here the coefficients

$$\lambda_a = \frac{\sqrt{k_i^a(k_i^a+k_c)}}{V_s\,\sigma_0}, \quad w_a = \ln\frac{T}{k_i^a + k_c}, \quad \lambda_{00} = \frac{k_i^0}{v_0\,\sigma_0}, \quad \lambda_p = \frac{A_D(T)}{A_D(T_s)}$$

$$\beta_* = \frac{V_s\,\sigma_0}{k_i^a+k_c}\sqrt{\frac{T}{T_s}}, \quad \beta_{1,2} = \frac{v_a^{1,2}}{V_s^s}, \quad \lambda_z = \sqrt{\frac{k_i^z}{A_D(T_s)}\frac{1}{\sigma_0}}$$

depend only on the plasma temperature.

Eq.(14c) is an integral of Eq.(3), obtained with taking into account of the condition (6a). In the new variables the other boundary conditions (6b)-(9) have the following form:

$u=0$

$$\frac{v_a^1}{V_s}\eta_a^1 = (1+\eta_a^*)(1-R_N), \quad \frac{v_a^2}{V_s}\eta_a^2 = (1+\eta_a^*)R_N$$

$$\eta = \alpha^s \frac{d\eta}{du}, \quad \eta_z = \alpha_z^s \frac{d\eta_z}{du} \tag{15}$$

$$\eta\frac{dT}{du} = \varepsilon_D(\gamma_s-\alpha)T\frac{d\eta}{du}$$

$u=u_0$

$$\eta_a = \eta_{0\leq z\leq z_U} = 0 \tag{16a}$$

$$\eta = \eta_b \equiv \frac{A_D(T_s)\,\sigma_0\,n_b}{\Gamma_s}, \quad \frac{dT}{du} = \frac{q_0}{\kappa_\perp\,n_b\,\sigma_0} \tag{16b}$$

where $\alpha^s=V_*/(A_D\sigma_0)$, $\alpha_z^s=V_*^z/(A_D\sigma_0)$.

Besides (15) Eqs(14) have an additional boundary condition - $\eta(0)=A_D(T_s)\sigma_0/V_*$ - and for determination of $\eta_0(u)$, $\eta(u)$, $\eta_z(u)$, T(u) only the second condition of (16b) is enough.The first one is necessary to determine Γ_s and to obtain the profiles of dimensional densities with given n_b. It is remarkable that the profiles $\eta_0(u)$, $\eta(u)$, $\eta_z(u)$, T(u) and the radiative potential can be calculated if instead of (16b) one sets the plasma temperature at the LCMS.

3.2. The radiative potential.

The integration of Eq.(5) gives the plasma heat balance in the peripheral region as a whole:

$$q_0 = \Gamma_s \left(\gamma_s T_s + E_i + S_l E_A\right) \tag{17}$$

here

$$E_A = \int_0^{x_0} dx \sum_{1 \le z \le zLi} n_z \, n \, L_z$$

is the energy losses by electrons on the ionization and excitation of an impurity particle coming into the discharge. In Ref.[2] this value was called the "radiative potential". In the dimensionless variables one has[32]:

$$E_A = \int_0^{u_0} \sum_{1 \le z \le_{Li}} L_z(T(u))\eta_z(u) \frac{du}{v_0 \sigma_0}$$

As it was shown above the profiles η_z(u), T(u) are determined simply by T_s value. Hence the radiative potential depends on the discharge conditions only through the temperature at the LCMS and the parameters $\sigma^s, \alpha_z^s, \gamma_s$, A_D, ε_d, η (0), which are external ones for a model of the peripheral region.

The scheme of E_A calculation is the following. We set a certain initial profile T(u) and Eqs.(14a)-(14d) are solved numerically by the method of factorization[21]. Then the obtained solution are used to calculate the next approximation of T(u) from Eq.(14e). The convergence of iterations is high enough - a difference between the fourth and fifth ones is smaller than 5%. With $u_0 > 5$ the value of E_A is practically independent of u_0. The results change weakly with magnitudes of σ^s, α_z^s, γ_s, $\eta(0)$.

In Fig.4 curves 1,2 present the dependences of E_A on T_s for carbon and oxygen, respectively, calculated with $\sigma^s = \alpha_z^s = 0.15$, $\varepsilon_D = 0.4$, $A_D = 10^{17} cm^{-1} s^{-1}$, $\gamma_s = 8$, $S_l = 0.02$. These magnitudes were found from the best coincidence of the calculated profiles of n and T with the measured ones under typical conditions of Ohmic discharges in TEXTOR[22]. The experimental data of Ref.[2] are given by crosses and curve 3 demonstrates the results of our calculation for the ratio of carbon and oxygen influxes into the discharge equal 2 and $S_l^c + S_l^o = 0.03$.

E_A increases sharply when the plasma temperature at the LCMS becomes smaller a certain value. In order to understand this we consider the following simple model. Let's assume that T is close to T_s in the entire peripheral region. Summarizing all Eqs.(14d) with $z \le z_{Li}$ one has:

$$\frac{d^2\eta_\Sigma}{du^2} = -\lambda_0^2\eta_0 + \lambda_{z_{Li}}^2\eta_{z_{Li}} \tag{18}$$

where

$$\eta_\Sigma = \sum_{1\le z\le z_{Li}} \eta_z$$

The first term in the right hand side of Eq.(18) describes an appearance of impurity ions due to the ionization of neutrals, the second one - the ionization into the weakly radiating helium-like state. Since $\lambda_z \ll \lambda_{z-1}$ with $T_s \ll I_z$ lithium-like ions penetrate into the plasma more deeply than the ions with $z < z_{Li}$. Thus for an estimate one can presume $\eta_\Sigma \approx \eta_{zLi}$ in the whole peripheral region. According to (14b) $\eta_0 = \exp(-\lambda_{00}u)$ and with $\alpha_z^s \ll 1$ one has from Eq.(18)

$$\eta_{z_{Li}} \approx \eta_\Sigma \approx \frac{\lambda_0^2}{\lambda_{00}^2}\,[\,\exp(-\lambda_{z_{Li}}u) - \exp(-\lambda_0 u)] \tag{19}$$

Thus the density of strongly radiating ions increases on the ionization length of neutrals and then decreases on the ionization length of lithium-like ions. Substituting (19) into the expression for E one has:

$$E_A = \frac{v_0\, L_{z_{Li}}}{k_i^o\sqrt{k_i^{zLi}A_D}} \tag{20}$$

Since the temperature dependences of L_{zLi} and k_i^0 practically compensate each other $E_A \sim \exp(I_{zLi}/2/T_s)$. Thus the increase of E_A with a drop of T_s results from a deeper penetration of strongly radiating ions into the plasma. The formula (20) gives a qualitative agreement with the calculation results.

3.3.Transition into the state with "detached plasma".

With taking into account of the conditions (16b) the plasma heat balance in the peripheral region (17) can be rewritten in the following form:

$$\frac{q_0}{n_b} = \frac{A_D(T_s)\,\sigma_0}{\eta_b(u_0)}\,(\gamma_s T_s + E_i + S_I\,E_A) \equiv F(T_s) \tag{21}$$

For several impurity species, entering into the discharge, $S_I E_A = \Sigma S_I^j E_A^j$, where S_I^j is the partial erosion coefficients.

There is a function of T_s on the right-hand side of Eq.(21), which is shown in Fig.5 for a case of carbon and oxygen influxes into the plasma with $S_I^c = 0.02$, $S_I^o = 0.01$. Here we have shown also the parts of F, corresponding to the energy losses with charged particles into the SOL and on the ionization and excitation of deuterium neutrals, $F_c = A_D\sigma_0(\gamma_s T_s + E_i)/\eta_b(u_0)$, and with impurity radiation, $F_r = A_D\sigma_0 S_I E_A/\eta_b(u_0)$.

The left hand side of Eq.(21) is inversely proportional to the ratio of the mean electron and current densities in the discharge ρ. Indeed for ohmic discharges $q_0 = I_p V_L/(4\pi^2 aR)$, where I_p is the plasma current, V_L is the loop voltage, a, R are the minor and major radii of the plasma column, and

$$\frac{q_0}{n_b} \approx \frac{V_L}{\rho}\,\frac{a}{4\pi R}$$

According to Ref.[22,23] the onset of MARFE's or a "detached plasma" occurs in ohmic discharges when ρ exceeds a certain critical value ρ_c. An analogous conclusion can be drawn from Fig.6: if q_0/n_b is smaller than the minimum value of F, i.e. ρ is larger than $\rho_c^t = V_L a/(4\pi R F_{min})$, any stationary stable state with moderate radiative losses doesn't exist i.e. detachment takes place. Magnitudes of ρ_c do not differ strongly for different devices and are in a range of $4 \div 7 \cdot 10^{11} A^{-1} cm^{-1}$[22,23]. Assuming $V_L = 1V$, $a/R = 0.4$ one has $\rho_c^t \approx 7 \cdot 10^{11} A^{-1} cm^{-1}$ in good agreement with the experimental data. It is interesting to note that earlier[12] the same result was obtained on the basis of a much simple model, under the assumption of coronal equilibrium for impurities[13].

The onset of a "detached plasma" results in a contraction of the discharge and in a dramatic changing of the plasma parameter profiles. The calculated profiles of the plasma density, temperature and the power density of radiative losses are presented in Fig.6-8 for ohmic discharges in TEXTOR(I_p=340kA, V_L=0.9V) for different n_b. The state with "detached plasma" takes place with the highest density - nearly 90% of a net power, transported to the peripheral region is radiated from the layer, which is shifted to the center of the plasma - Fig.8. Contraction of the plasma density profile results from a deeper penetration of deuterium atoms into the discharge with a reduction of T_s lower than the hydrogen ionization potential. Experimentally such an evolution of density and temperature was observed in TORE SUPRA also[24].

Fig.9 shows radiation level $\alpha_r = \Gamma_s S_I E_A / q_0$ as a function of n_b, calculated and measured in TEXTOR [2] for two different magnitudes of the plasma current (the corresponding values of q_0 are 0.8 (the curve 1 and diamonds) and 1.06 W/cm^2 (2,triangulares)).

4. AUXILIARY HEATING.

4.1.Transport coefficients.

Plasma confinement usually deteriorates in limiter tokamaks when additional heating is applied[25]. This is manifested in an essential increase of neutral fluxes from the limiter. In TEXTOR[25,26] the particle confinement time τ_p is by $3 \div 4$ times lower on the NI stage that on the OH one. This change in transport is modelled by an introduction of additional items D_*, κ_* in the transport coefficients (13). Some models have been proposed, which have pretensions to explain the dependences of κ_* on the plasma parameters. From our point of view the approach, elaborated in Ref.[27], is the most well-founded one. It is based on the idea of destabilisation of convective cells, produced by regular drift waves. According to Ref.[27]

$$\kappa_{\circ} = \alpha_{\circ} \frac{n\, c_s^3}{\omega_i^2} \frac{d\ln n}{dx} \tag{22}$$

where $\alpha_{\circ}$ is a numerical factor, $c_s=(T_e/m_i)^{1/2}$ is the ion sound velocity, $\omega_i=eB/(m_ic)$ is the ion Larmor frequency.

Diffusion of charged particles is a more complicated process than heat conduction and till now there isn't any reliable theory for particle transport in the discharges with auxiliary heating. Therefore we try to connect $D_{\circ}$ with τ_p analytically and to determine from the measured dependences of τ_p on net power and mean plasma density how $D_{\circ}$ depends on the plasma parameters.

Let us assume that $T=T_s$ in the region where neutrals are ionized. We consider discharge modes with negligible impurity radiation and search for $D_{\circ}$ in the following form: $D_{\circ}=An^{\alpha}T^{\beta}$. The plasma flux across the LCMS can be estimated as follows[28]: $\Gamma_s \approx \langle\langle D_\perp \rangle\rangle n_b/l_{\circ}$, where $\langle\langle D_\perp \rangle\rangle$ is the averaged diffusivity in the region under consideration, $l_{\circ}$ is its characteristic width. As follows from (14a), (14c) $l_{\circ} \approx 1/(\sigma_{\circ}\langle\langle n \rangle\rangle)$ where $\sigma_{\circ} \approx \lambda_a \sigma_0 \approx (k_i^a(k_i^a+k_c))^{1/2}/V_s$ depends on the plasma temperature very weakly (with T change in the range of $15\div100$ eV $\sigma_{\circ}$ deviates from $7\cdot10^{-15}$cm^2 not more than by 15%), $\langle\langle n \rangle\rangle \approx n_b/2$. T_s is estimated from (17b) assuming $q_\perp \approx q_0$.

Finally for $\tau_p=n_ba/(2\Gamma_s)$ one obtains

$$\tau_p \approx a \left[\frac{2^{\alpha-\beta}\, n_b^{\beta-\alpha-1}}{A\, \sigma_{\circ}} \left(\frac{\gamma_s}{q_0}\right)^{\beta} \right]^{\frac{1}{1+\beta}} \tag{23}$$

According to the experimental data [26] τ_p changes in inverse proportion to square root of the power or q_0. This means that ß must be equal to 1. Besides, τ_p is practically independent of the density for $\langle n \rangle \gtrsim 2.5\cdot10^{13}$cm^{-3}. Hence $\alpha=ß-1=0$. Thus the dependence of $D_{\circ}$ on the plasma parameters is analogous to Bohm diffusion $D_B=cT/(16eB)$. Moreover the magnitude of $D_{\circ}$ is numerically close to D_B. With $\gamma_s=10$, $q_0=5.5$W/cm^2 (the net power 1.8 MW) and $A=c/(16eB)$ by 2.25T $\tau_p \approx 12.5$ms in agreement with experiment[26].

Henceforth we assume $D_{\circ}=D_B$. In order to avoid an unrealistically strong increase of $D_\perp$ to the discharge centre the magnitude of $D_{\circ}$ is restricted by D_B value at a certain temperature $T_{\circ}$. The calculation results depends on $T_{\circ}$ magnitude relatively weak when $T_{\circ} \geq 100$ eV.

4.2. The calculation results and their interpretation.

Here we present the results of our modelling of TEXTOR discharges with additional heating by neutral injection and with neon puffing[2,8]. The calculation has done with $q_0 = 5.5 W/cm^2$, which corresponds to the total heat flux to the peripheral region of 1.8 MW; besides neon, carbon atoms are released into the plasma with $S_l = 0.03$, $v_0 = 5 \cdot 10^5 cm/s$; in formula (22) $\alpha_* = 2.5$. Fig.10 shows how the radiation level α_r depends on neon concentration $c_{Ne} = \Sigma n_z/n$ at the border between the central and peripheral parts of the discharge($x = x_0$). The different curves correspond to different magnitudes of n_b.

The heat flux into the SOL decreases with increase in c_{Ne} owing to diminution both of the plasma temperature at the LCMS and of the charged particle flux into the SOL. This is demonstrated in Fig. 11 and 12, where the dependences of T_s and τ_p on α_r are presented for different n_b. In order to understand such their behaviour we analyze the changing of some parameters with an increase in c_{Ne}. Fig.13 presents the profiles of the density of radiative losses with $n_b = 5.6 \cdot 10^{13} cm^{-3}$ and different α_r. There are two maxima in the radiation profiles. The first one is in the vicinity of the LCMS and connects with carbon radiation. The second one occurs at a distance of 8 cm from the LCMS and corresponds to radiation of neon. The strongest changes in the temperature and diffusivity occurs in the region, located nearer to the LCMS than the second maximum of Q_{rad} - see Fig.14,15. This strongly influences the deuteron flux since their source is also localized in this part of the discharge periphery as follows from the Fig.16, where the profiles of their source density $S_i = k_i^a n n_a$ are presented.

An increase of α_r up to 90% does not result in any substantial displacement of Q_{rad} maximum to the discharge centre, i.e the plasma does not detach. To understand this fact let's analyze the function $F(T_s)$, defined by the expression (21). For the case under consideration ($D_* = D_B$) and neon as an impurity, F is presented in Fig.17 with $n_b = 5.6 \cdot 10^{13} cm^{-3}$ and different c_{Ne}. The stationary magnitudes of T_s are determined by the points of intersection of the line $p(T_s) = q_0/n_b$ and the graphs of $F(T_s)$. F is a monotonic function of T_s for all values of neon concentration. Thus with an increase in C_{Ne}, one can realize discharge modes without "detached plasma" and with a heat flux into the SOL smaller than 10% of q_0 (the curve 6 gives the ratio of this flux to n_b).

The neon concentration, which is necessary to radiate 90% of net power, depends on n_b and q_0 as it is shown in Fig.19. In TEXTOR-U with a reactor level of q_0 of 20 W/cm^2 and $n_b \sim 10^{14} cm^{-3}$ a state with such a radiating periphery is feasible with c_{Ne} not larger than 1%.

4.3. Comparison with experiment.

In TEXTOR[8] radiation of 90% of a net power is attainable with a neon concentration in the discharge centre of 0,5%. According to Fig.19 the calculations give a similar value of 0.75%. The corresponding ratio of the neon and deuterium atom fluxes from the limiter equals 0.036, which agrees with the measured concentration of neon ions in the SOL ~4%.

Spectroscopic data[7] show that the maximum of Ne^{7+} ion radiation is located in the discharge region where $T_e \approx 140$ ev. An analogous conclusion can be drawn from Fig.14 and Fig.19, where the profiles of the densities of neon ions with $z = 1 \div 7$ are shown for the case of $n_b = 5.6 \cdot 10^{13} cm^{-3}$, $c_{Ne} = 0{,}75\% (\alpha_r = 0.906)$. But contrary to the conclusion of Ref.[7] that Ne^{7+} ions give a main contribution in the radiative energy losses, the calculations show that Ne^{6+} ions radiate more intensively. This follows from Fig.20, presenting the profiles of power densities of radiative losses $Q_z = nn_zL_z$ for different ions. It is noteworthy that according to Fig.4 of Ref.[7] the maximum of Ne^{7+} radiation is shifted also more deeply into the discharge than the maximum of the total radiative losses.

Since the calculated data thus agree on the whole with the experimental results, the proposed model gives an adequate description of the processes of energy and particle transport in the discharges with additional heating and neon puffing.

5. CONCLUSIONS.

1. The proposed one-dimensional model of particle and energy transport in the peripheral region of a tokamak allows one to describe discharge modes with strong impurity radiation in agreement with experimental data.
2. The simple approximate formulas, derived for the dependences of energy radiative losses of impurities on the electron temperature, simplify calculations essentially.
3. In ohmic discharges:
the radiative potential - net energy losses by electrons on the ionization and excitation of an impurity particle, coming into the plasma, - depends mainly on the electron temperature at the last closed magnetic surface T_s, what results from the inversely proportionality of the diffusivity to the plasma density (neo-Alcator scaling);
the transition into the state with "detached plasma" occurs when with a changing of T_s the ratio of total energy losses in the peripheral region to the plasma density at the border with the discharge core passes through its minimum value.
4. In the discharges with auxiliary heating and deteriorated confinement:
particle transport in the peripheral region can be described by Bohm diffusion;
with puffing of neon, more than 90% of the power transported to the discharge periphery can be radiated without the onset of "detached plasma".

Acknowledgments

The author would like to thank Dr. U.Samm and Dr. H.A.Claassen for fruitful discussions of different topics concerning impurity transport and radiation and Prof. E.Hintz for making possible to work in IPP during the spring of 1991, when this investigation was started. Partly this work has been done under the financial support of the A. von Humboldt Foundation.

6.SUPPLEMENT

1. Energetic spectrum of neutrals, coming from a limiter.

An interaction of deuterium ions with the limiter surface results in the reflection of some part of them as atoms with an energy of T_s. With $T_s = 40$ eV and in the case of a carbon surface the reflection coefficient $R_N \approx 0.3$ and increases with a decrease of temperature[29]. When the surface is saturated with gas the absorbed particles desorbs as molecules with a thermal velocity of 10^5cm/s. These molecules are dissociated and ionized by electrons at a distance from the limiter of 0.5 cm and as a result deuterium ions and atoms appear with a kinetic energy of 1 eV. With the electron temperatures lower than 20 eV dissociation of molecules prevails and we do not take their ionization into account. In any case this does not give a large error because the deuteron source due to the molecular ion dissociation doesn't differ principally from that one due to ionization of Franck-Condon atoms since both are located much closer to the LCMS than the source due to ionization of charge-exchanged atoms.

2. Diffusive approximation for charge-exchanged atoms.

A diffusive approximation can be applied when $k_i^a \ll k_c$ and the temperature gradient is not very sharp. In our case, the first condition only loosely satisfies - $k_i^a < k_c$ with all T. But the used form of D_a, derived in Ref.[8] from a kinetic equation, allows to describe correctly an opposite limit case of $k_i^a \gg k_c$. Indeed in such a case it follows from Eq.(1) and the formula for D_a that the characteristic length of the density decay of charge-exchanged atom is the same as in a kinetic approximation - $V_s/(k_i^a n)$.

3. Transparency of the SOL for neutrals.

The plasma parameters in the SOL depend strongly on the discharge conditions. In Ohmic discharges $T \leq 20$ eV, $n \leq 3 \cdot 10^{12}$cm^{-3}, in the discharges with auxiliary heating $T \leq 40$eV, $n \leq 10^{13}$cm^{-3}. In the both cases the path length of Franck-Condon atoms before ionization $l_i = v_a/(k_i^a n)$ is longer that 5cm, for charge-exchange atoms $l_i > 10$ cm. For carbon and oxygen particles with $v_0 = 5 \cdot 10^5$cm/s $l_i^c > 4$ cm and $l_i^o > 8$ cm, respectively, in ohmic discharges and $l_i^c > 0.6$cm and $l_i^o > 1$cm in the additionally heated discharges. Neon atoms, reflected from the limiter, with a velocity of V_s have $l_i^{Ne} > 10$ cm. A decay length of the electron density in the SOL is of $2 \div 3$ cm. Thus the SOL is always transparent for deuterium and neon atoms and for carbon and oxygen neutrals in ohmic discharges. In the case of auxiliary heating the SOL can be opaque for the latter particles but these impurities do not play an important role enough in the energetic balance of the peripheral plasma.

4. Applicability of a one-dimensional model for the peripheral plasma.

With a localizing of the neutral particle source in a toroidal or a poloidal directions, for example, in a limiter configuration, the transport of charged particles, momentum and energy has a two-dimensional pattern - along and perpendicular to magnetic surfaces. In the case of toroidal limiter the equations of the continuity, thermal balance and motion along the magnetic field have the following form (without taking into account of drift effects)[13]:

$$\frac{\partial \Gamma_\perp}{\partial x} + \frac{\partial \Gamma_\parallel}{\partial l} = S \tag{S1}$$

$$\frac{\partial q_\perp}{\partial x} + \frac{\partial q_\parallel}{\partial l} = Q \tag{S2}$$

$$\frac{\partial}{\partial x}(\Gamma_\perp m_i V_\parallel) + \frac{\partial}{\partial l}(m_i n V_\parallel^2 + P) = Q \tag{S3}$$

where $dl = aB_T/B_\vartheta d\vartheta$, ϑ is the poloidal angle, $\Gamma_\parallel = nV_\parallel$, $V_\parallel$, $q_\parallel$ are the velocity and particle flux density along B, $P = n(T_i + T_e)$ is the plasma pressure, the terms S, Q, F describes an interaction of charged particle with neutrals and impurities.

An averaging of Eqs.(S1), (S2) over the magnetic surfaces give Eqs.(3), (5) but before using them it is necessary to ensure that everywhere on a surface the plasma parameters are close to the averaged ones. The characteristic change of temperature ΔT along B can be estimated from the equality of a heat flux into the region near the limiter due to electron heat conductivity, $Q_\parallel$, and an energy loss here. In the discharges with strong radiation of impurities the latter is close to the total power launched into the plasma $W = 4\pi^2 aRq_0$. For $Q_\parallel$ one has the estimate

$$Q_\parallel \approx \frac{\kappa_\parallel \Delta T}{L_\parallel} \sin\psi \; 2\pi R \delta_r$$

where $\kappa_\parallel = A_\kappa T^{2.5}$ is the longitudinal heat conductivity of electrons, $A_\kappa \approx 1.5 \cdot 10^{20} \text{cm}^{-1} \text{s}^{-1} \text{ev}^{-2.5}$, $L_\parallel = \pi qR$ is a connection length, $\sin\psi = a/(qR)$, ψ is a pitch angle of the magnetic field to the toroidal direction, δ_r is the characteristic width of the peripheral region. From the equality of $Q_\parallel$ and W one has

$$\frac{\Delta T}{T} \approx \frac{2(\pi qR)^2 q_0}{\kappa_\parallel \; \delta_r \; T}$$

A characteristic plasma temperature in the radiative region is of 30eV in ohmic discharges ($q_0 \approx 1\text{W/cm}^2$) and 100eV in auxiliary heated discharges ($q_0 = 5.5\text{W/cm}^2$), $\delta_r \approx 10$cm. This gives for TEXTOR condition ($a = 46$cm, $R = 175$cm, $q = 4$) $\Delta T/T \approx 0.3$ and 0.03 respectively.

From Eq.(S3) it is possible to estimate a plasma pressure change on the magnetic surface:

$$\frac{\Delta P}{P} \approx \left(\frac{V_\parallel}{V_s}\right)^2$$

$V_\parallel$ can be evaluated from Eq.(S1):

$$\frac{\Gamma_s}{\delta_r} \approx \frac{n V_\parallel}{L_\parallel}$$

Therefore

$$\frac{\Delta P}{P} \approx \left(\frac{\Gamma_s L_\parallel}{\delta_r n V_s}\right)^2 \approx \left(\frac{a\, L_\parallel}{2\delta_r \tau_p V_s}\right)^2$$

Both for ohmic and additionally heated discharges ($\tau_p \approx 40$ms and $\tau_p \approx 10$ms, respectively) we have $\Delta P/P < 0.01$.

Thus relative changes of the plasma temperature, pressure and density, consequently, along the magnetic surfaces are small and a one-dimensional description can be applied.

5. Pinch-effect.

Modelling of the transport of particles, puffed into the discharge, shows that in order to explain the time of their penetration into the plasma centre it is necessary to introduce an anomalous convection with a velocity V_p of 5m/s [30]. But for conditions of the peripheral region convective transport is negligible. Indeed $V_p \ll D_\perp d(\ln n)/dx \approx D_\perp/\delta_r \approx 20 \div 40$m/s.

6. Plasma isothermality.

The condition that T_i and T_e be nearly equal in the peripheral plasma has been discussed in Ref.[12] and is reduced to the following:

$$q_0^3 \ll D_\perp\, n_b^4$$

where q_0 is W/cm^2, $D_\perp$ is in m^2/s and n_b is in 10^{13}cm^{-3}.
This holds for the considered conditions under consideration - $\langle n \rangle \geq 3\cdot 10^{13}$cm^{-3} in ohmic discharges and $\langle n \rangle \geq 4.4\cdot 10^{13}$cm^{-3} in auxiliary heated discharges.

7. Effect of impurity recombination.

Negligibility of the radiative, dielectronic and three-body recombinative processes for impurity in the tokamak peripheral region is shown in a number of papers (see Ref.[9]). The charge-exchange on deuterium neutrals can play a more essential role[31]. A cross-section of such a process, σ_c, is of $3\cdot 10^{-15}$cm^2 for carbon and oxygen ions. With a neutral density near the limiter of 10^{11}cm^{-3} the time till charge-exchange τ_c is of 500μs and is smaller than the ionization time of C^{3+}, $O^{3+} \div O^{5+}$ ions. But τ_c does not exceed the time of the ion residence in the vicinity of the limiter $\tau_\parallel \approx l_\parallel/V_\parallel$, where $l_\parallel$ is the length of the limiter in B direction. One can show that $\tau_c/\tau_\parallel \approx \sigma_*/\sigma_c > 2.5$. This means that the charge-exchange on deuterium neutrals is not a dominant process in the impurity particle balance and in the first approximation it can be neglected.

REFERENCES

[1] ITER CONCEPT DEFINITION, Vol. 2,IAEA, Vienna (1989).

[2] SAMM,U., Radiation control in a limiter tokamak, Rep. Jül-2378, Institut für Plasmaphysik, Forschungszentrum Jülich, Ass. EURATOM-KFA(1990).

[3] POST,D.E., JENSEN,R.V., TARTER,C.B., et al., Rep. PPPL-1352, Princeton Plasma Phys. Lab., Princeton(1977).

[4] KLEVA,R.G., DRAKE,J.F., DENTON,R.E., Comm. Plasma Phys. Contr. Fusion 13(1989)63.

[5] ULRICKSON,M., THE JET TEAM AND THE TFTR TEAM, J.Nucl.Mater. 176&177(1990)44.

[6] TOKAR,M.Z., NEDOSPASOV,A.V., YAROCHKIN,A.V., The possible nature of hot spots on tokamak walls, Nucl. Fusion. 32(1992)15.

[7] SAMM,U., BERTSCHINGER,G., BOGEN,P., et al., in Controlled Fusion and Plasma Heating (Proc. 18th Eur. Conf. Berlin, 1991), Vol.15C, Part III, European Physical Society (1991)157.

[8] SAMM,U., DIPPEL,K.H., BERTSCHINGER, G., et al., Helium exhaust in plasmas with strong radiative edge cooling, Abstract of a Rep. on 10th Conf. on Plasma Surface Interaction, Monterey(1992).

[9] CLAASSEN, H.A., GERHAUSER,H., Plasma Edge Physics: Theoretical Studies on Impurity Transport, Int. Rep. Institut für Plasmaphysik, Forschungszentrum Jülich, Ass. EURATOM-KFA(1991).

[10] POSPIESZCZYK,A., BAY.H.L., BOGEN,P., et al., J. Nucl. Mater. 145&147(1987)574.

[11] SAMM,U., KOSLOWSKI,H.R., SOLTWISCH,H., in Controlled Fusion and Plasma Heating (Proc.18th Eur. Conf. Berlin, 1991), Vol.15C, Part III, European Physical Society(1991),137.

[12] LEHNERT,B., Nucl. Fusion 8(1968)173.

[13] NEDOSPASOV,A.V., TOKAR',M.Z., in Problems of Plasma Theory, Vol.18 (KADOMTSEV,B.B., Ed.), Energoatomizdat, Moscow (1990) 68 (in Russian).

[14] BELL,K.L., GILBODY, H.B., HUGHES,J.G., et al., Atomic and molecular data for fusion, part 1, Rep. CLM-R216, Culham Laboratory, Abingdon Oxfordshire (1982).

[15] LENNON,M.A., BELL,K.L., GILBODY, H.B., et al., Atomic and molecular data for fusion, part 2, Rep. CLM-r270, Culham Laboratory, Abingdon Oxfordshire (1986).

[16] ITIKAWA,Y., et al., Atomic Data and Nuclear Data Tables 33(1985)150.

[17] DAVIS,J., KEPPLE,P.C., BLAHA,M., J. Quant. Spectrosc. Radiat. Transfer 16(1976)1043.

[18] NAKAZAKI,S., HASHINO,T., J. Phys. B: At. Mol. Phys. 15(1982)2767.

[19] CHANG,C.C., GREVE,P., KOLK,K.H., KUNZE,H.J., Physica Scripta 29(1984)132.

[20] JANEV,R.K., POST, D.E., LANGER,W.D., et al., J. Nucl. Mater. 121(1984)10.

[21] DEMIDOVICH,B.P., MARON,I.A., SHUVALOVA,E.Z., Numerical methods of analysis, Nauka, Moscow (1967) (in Russian).

[22] SAMM,U., BAY,H., BOGEN,P., Properties of "detached"- plasmas, Rep. Jül-2123, Institut für Plasmaphysik, Kernforschungsanlage Jülich, Ass. EURATOM-KFA (1987).

[23] LIPSCHULTZ,B., J. Nucl. Mater. 145&147(1987)15.

[24] GROSMAN,A., EVANS,T.E., GHENDRIH,Ph., et al., Plasma Phys. Controlled Fusion 32(1990)1011.

[25] SAMM,U., BOGEN,P., HARTWIG,H., et al., in Controlled Fusion and Plasma Physics (Proc. 16th Eur. Conf. Venice), Vol.13B, part III, European Physical Society (1989) 991.

[26] BOEDO,J., GRAY,D., private communication.

[27] KADOMTSEV,B.B., Nucl. Fusion 31(1991)1301.

[28] NEDOSPASOV,A.V., TOKAR',M.Z., J. Nucl. Mater. 93&94(1980)248.

[29] BEHRISCH,R., ECKSTEIN,W., in Physics of Plasma-Wall Interaction in Controlled Fusion (POST,D.E., BEHRISCH,R., Ed.), Plenum Press, New York (1986)413.

[30] SRACHAN,J.D., CHAN,A., Nucl. Fusion 27(1987)1025.

[31] PHANEUF,R.A., JANEV,R.K., PINDZOLA,S., Rep.ORNL-6090, Oak/Ridge Nat.Lab., Oak/Ridge(1987).

[32] TOKAR,M.Z., in Controlled Fusion and Plasma Heating (Proc. 18th Eur. Conf. Berlin, 1991), Vol. 15C, Part III, European Physical Society (1991) 1.

[33] CLAAßEN,H.A., GERHAUSER,H., Impurity transport at the plasma edge: the transition from 2D to 1D models in axisymmetric toroidal systems and the role of poloidal source distributions, Rep. Jül.-2576, Institut für Plasmaphysik, Forschungszentrum Jülich, Ass.EURATOM-KFA(1992).

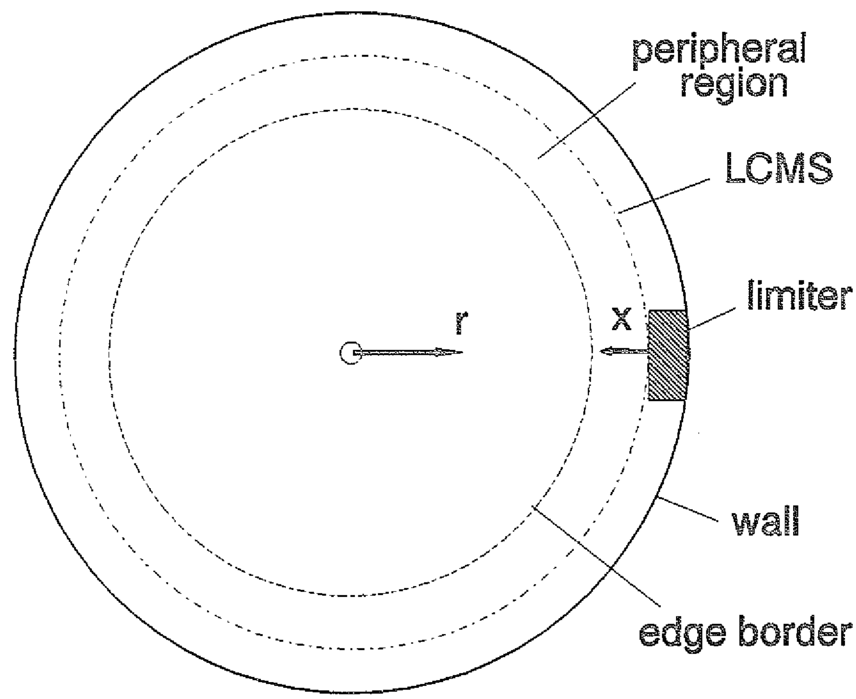

Fig.1 - A schematic view of the peripheral region in a tokamak with a toroidal limiter.

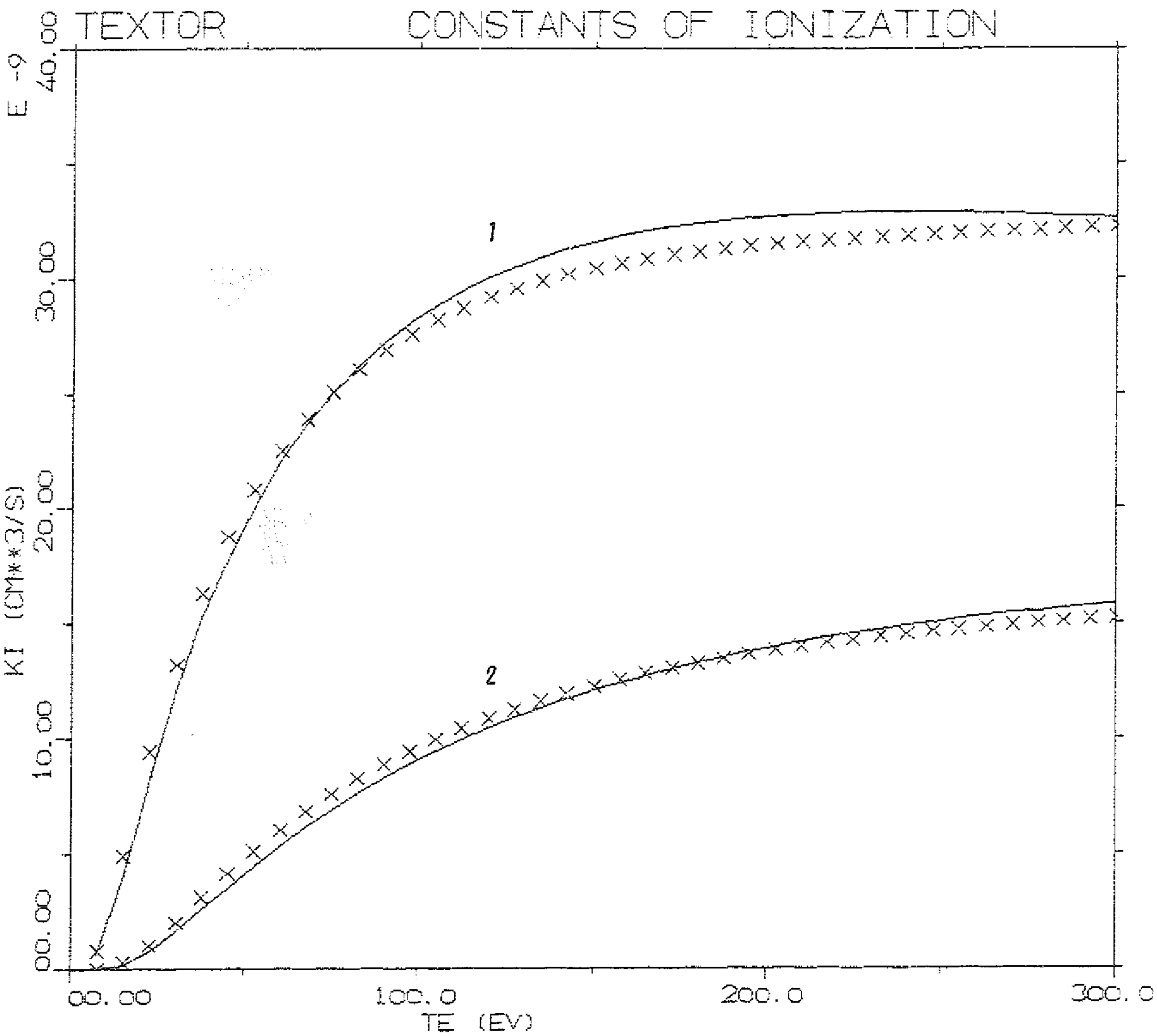

Fig.2 - Temperature dependences of the ionization constants of C^{+}(1) and O^{2+}(2) ions:
-- - calculations according to formula (10), × - Ref.[14] data.

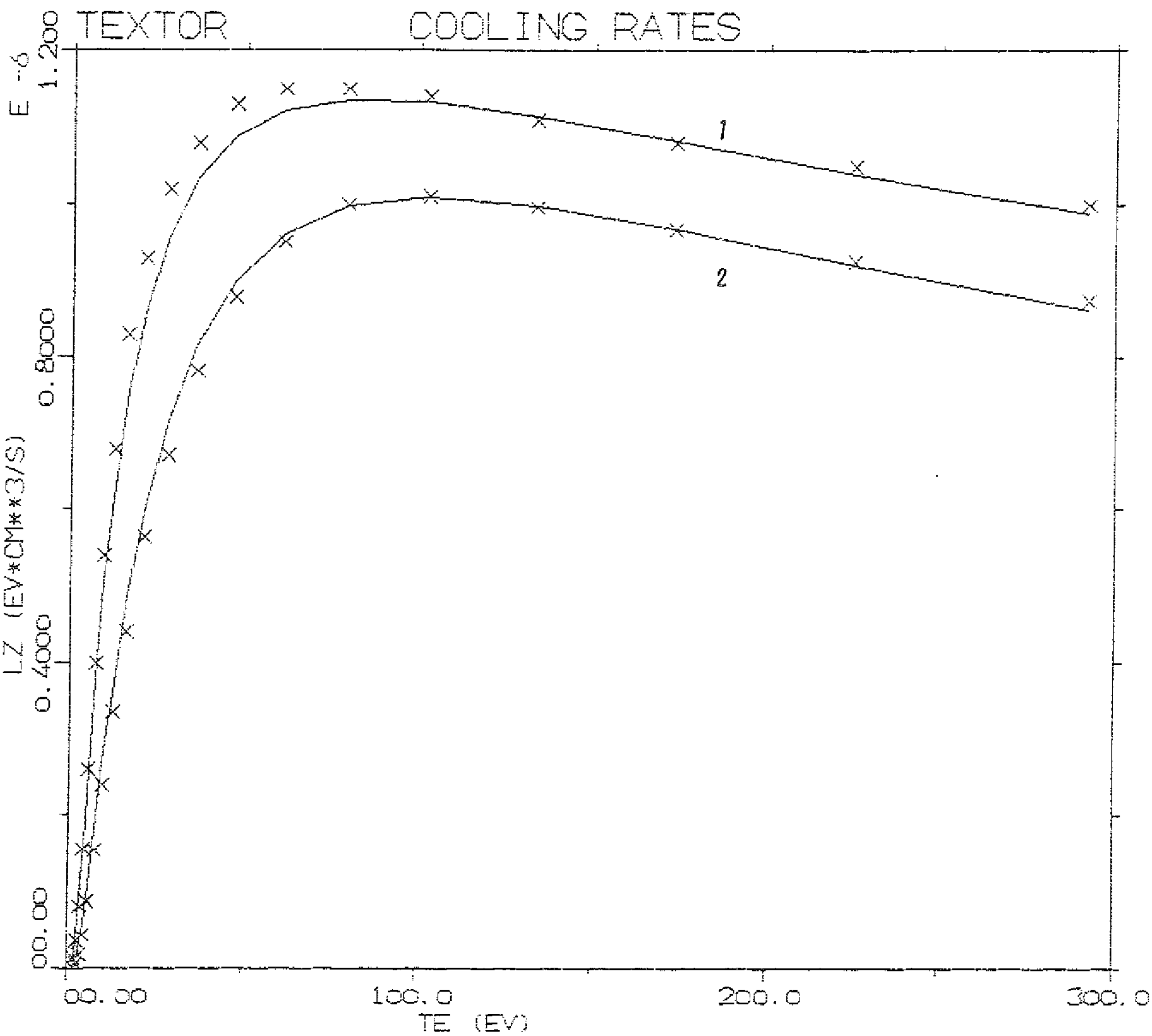

Fig.3 - Temperature dependences of the cooling rates of ions C^{2+}(1) and O^{4+}(2):
-- - calculations according to formula (12), × - Ref.[16] data.

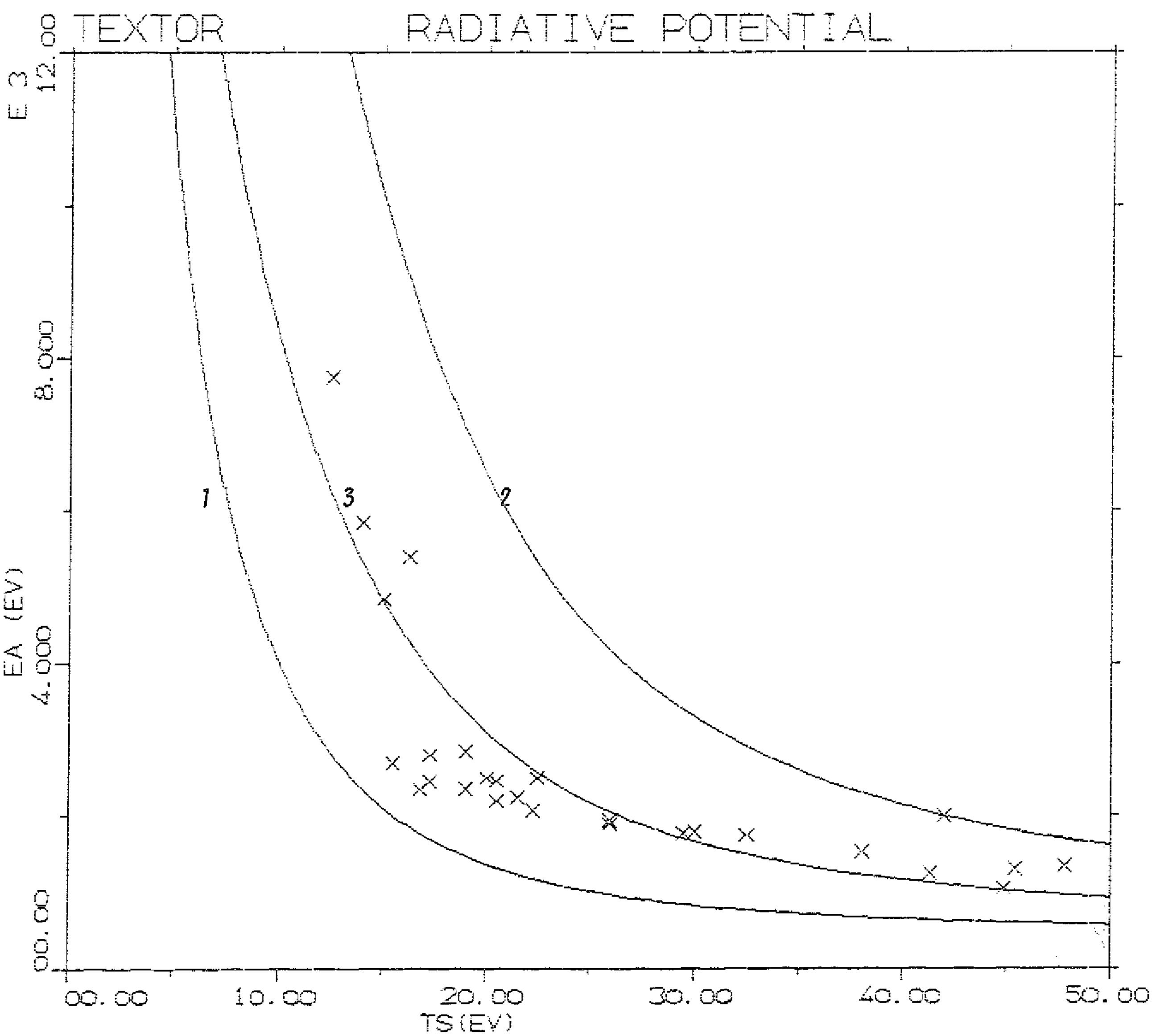

Fig.4 - Dependences of the radiative potential on the electron temperature at the LCMS:
-- - calculated results: pure carbon influx into discharge(1), pure oxygen influx(2),
mixture of carbon and oxygen influxes with ratio 2/1(3);
× - experimental data Ref.[2].

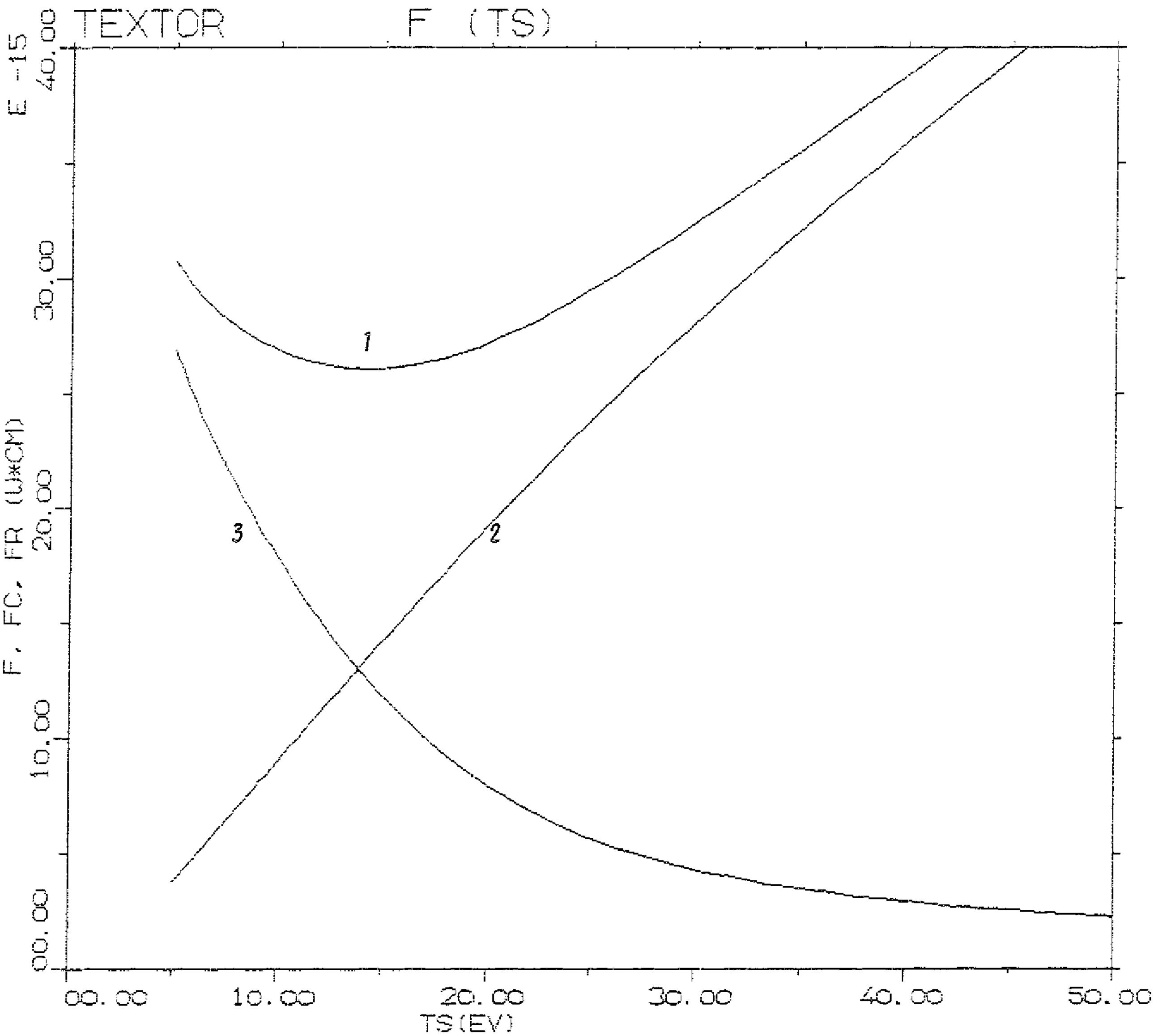

Fig.5 - 1 - Function $F(T_s)$ - the right-hand side of Eq.(21);
2 - F_c - the part of F, corresponding to the heat losses with particles into the SOL;
3 - F_r - the part of F, corresponding to radiative losses.

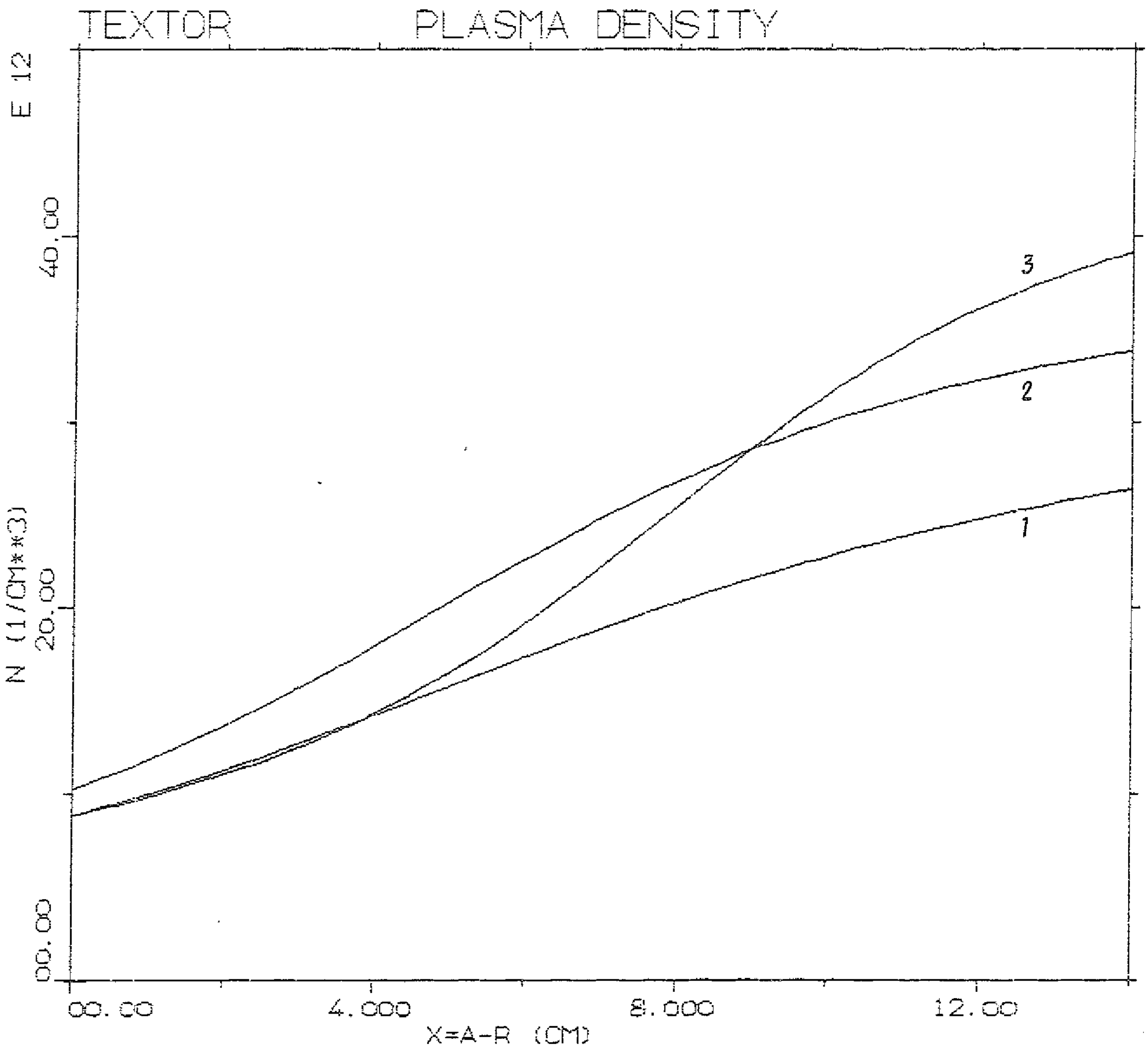

Fig.6 - Calculated profiles of the plasma density in ohmic discharge:
1 - n_b = $2.9 \cdot 10^{13} cm^{-3}$, 2 - n_b = $3.5 \cdot 10^{13} cm^{-3}$, 3 - n_b = $4.1 \cdot 10^{13} cm^{-3}$ ("detached plasma").

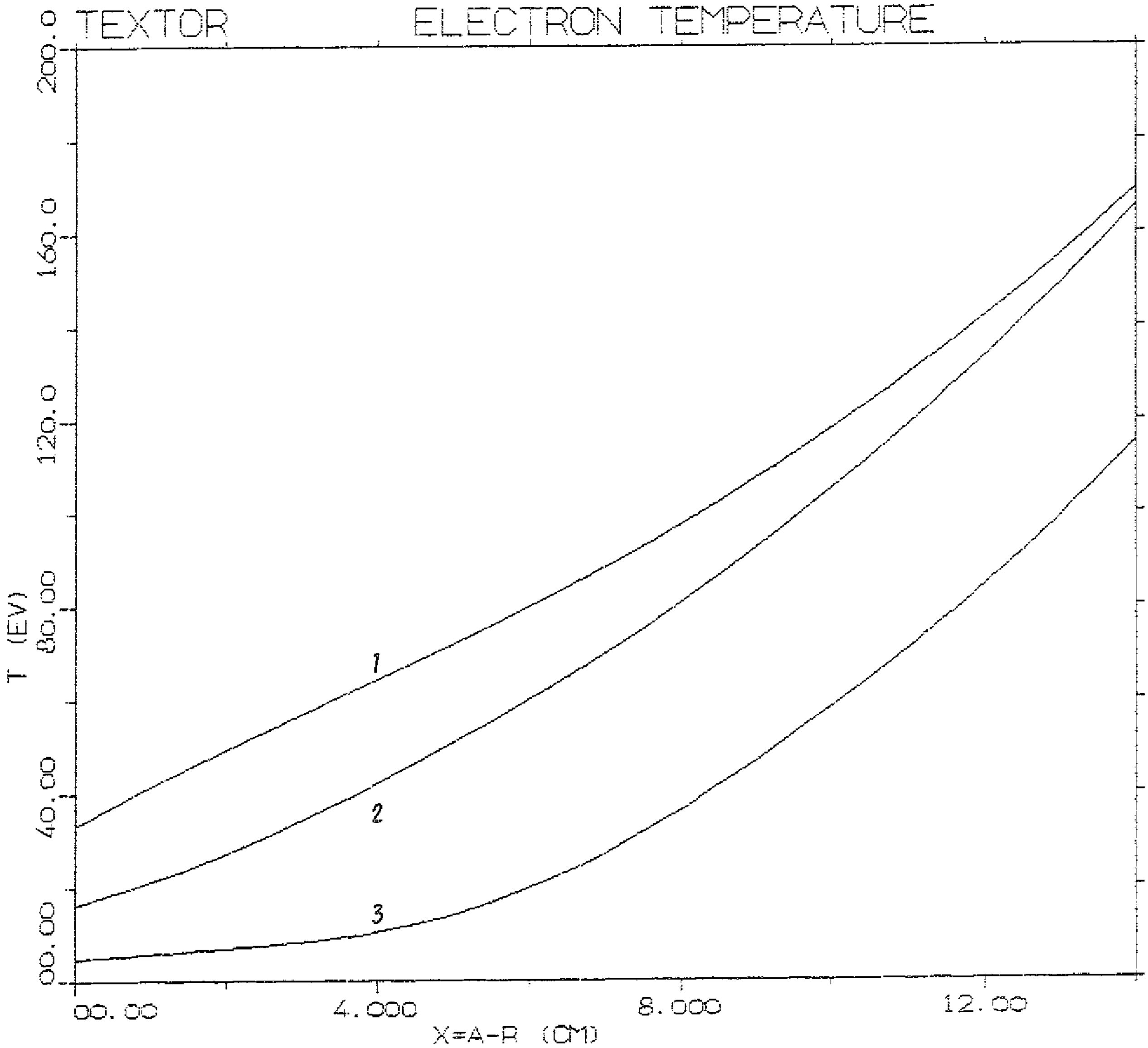

Fig.7 - Calculated profiles of the plasma temperature in ohmic discharge: 1 - $n_b = 2.9 \cdot 10^{13} cm^{-3}$, 2 - $n_b = 3.5 \cdot 10^{13} cm^{-3}$, 3 - $n_b = 4.1 \cdot 10^{13} cm^{-3}$ ("detached plasma").

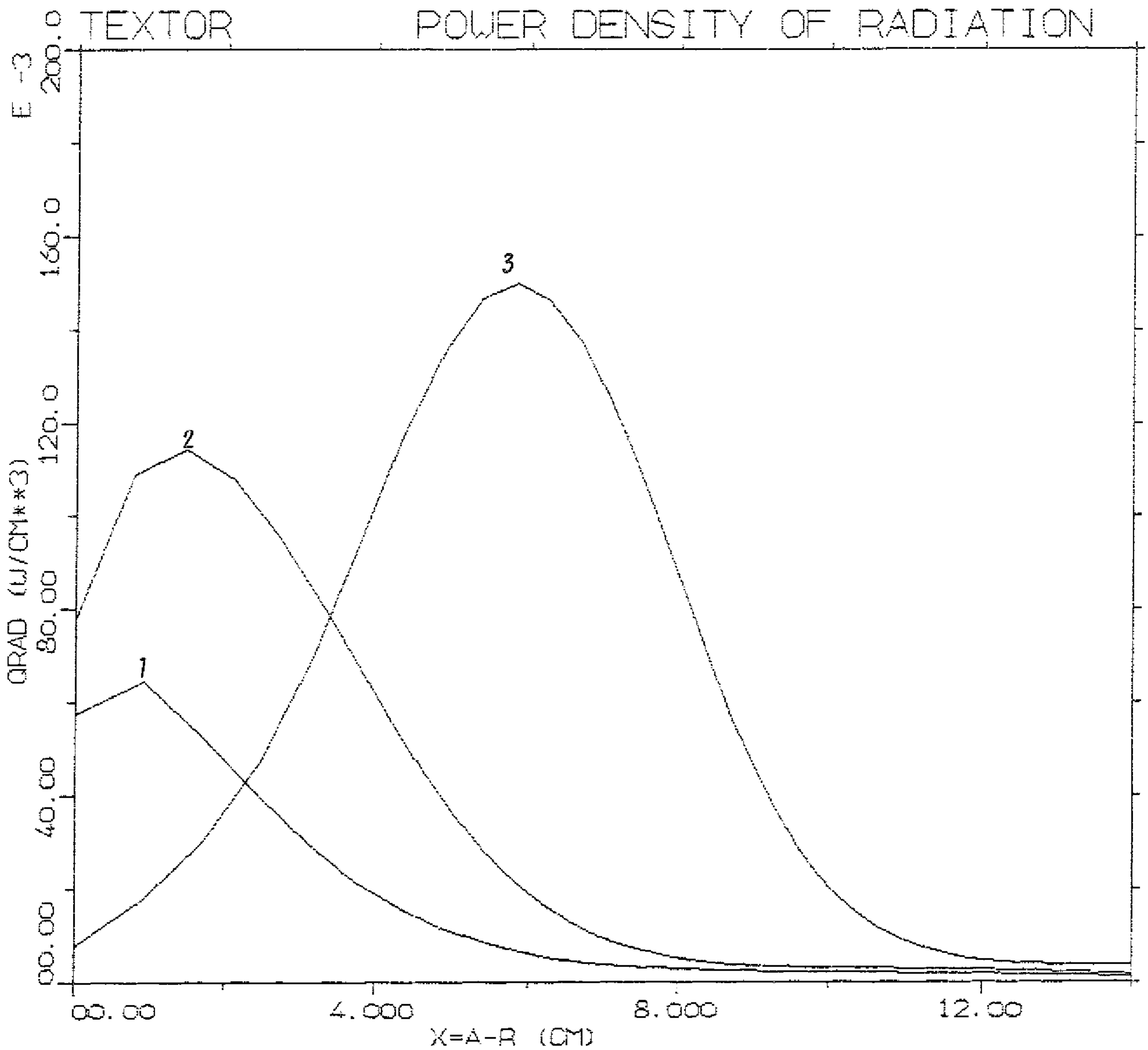

Fig.8 - Calculated profiles of the power density of the impurity radiation in ohmic discharge:
1 - $n_b = 2.9 \cdot 10^{13} cm^{-3}$, 2 - $n_b = 3.5 \cdot 10^{13} cm^{-3}$, 3 - $n_b = 4.1 \cdot 10^{13} cm^{-3}$ ("detached plasma").

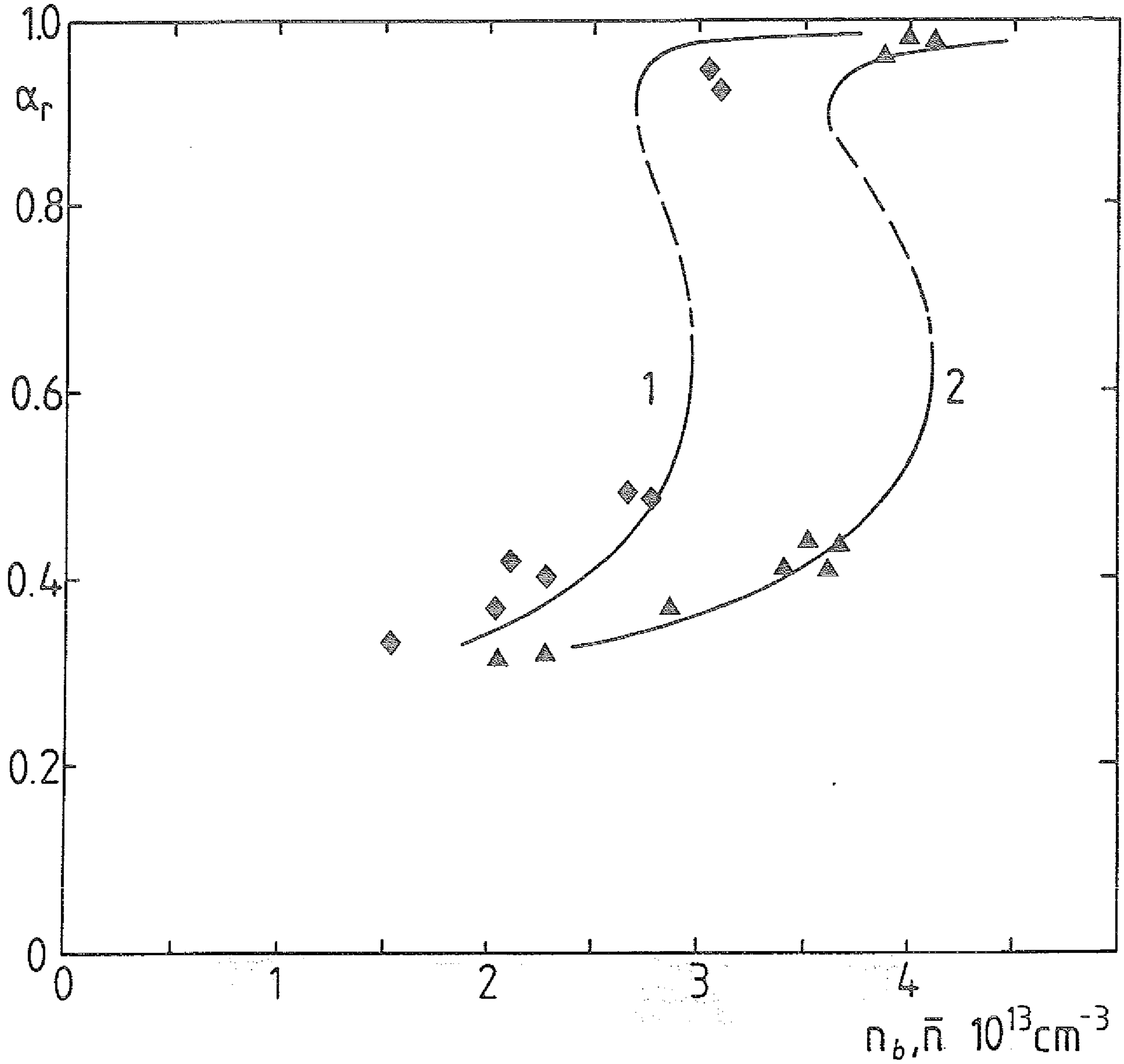

Fig.9 - Radiated part of the power launched into TEXTOR ohmic discharges - radiation level:
-- - calculated dependences on n_b, ◆, ▲ - experimental dependences on the mean density $<n>$.
(1, ◆ - for a plasma current of 260 kA; 2, ▲ - for 340 kA).

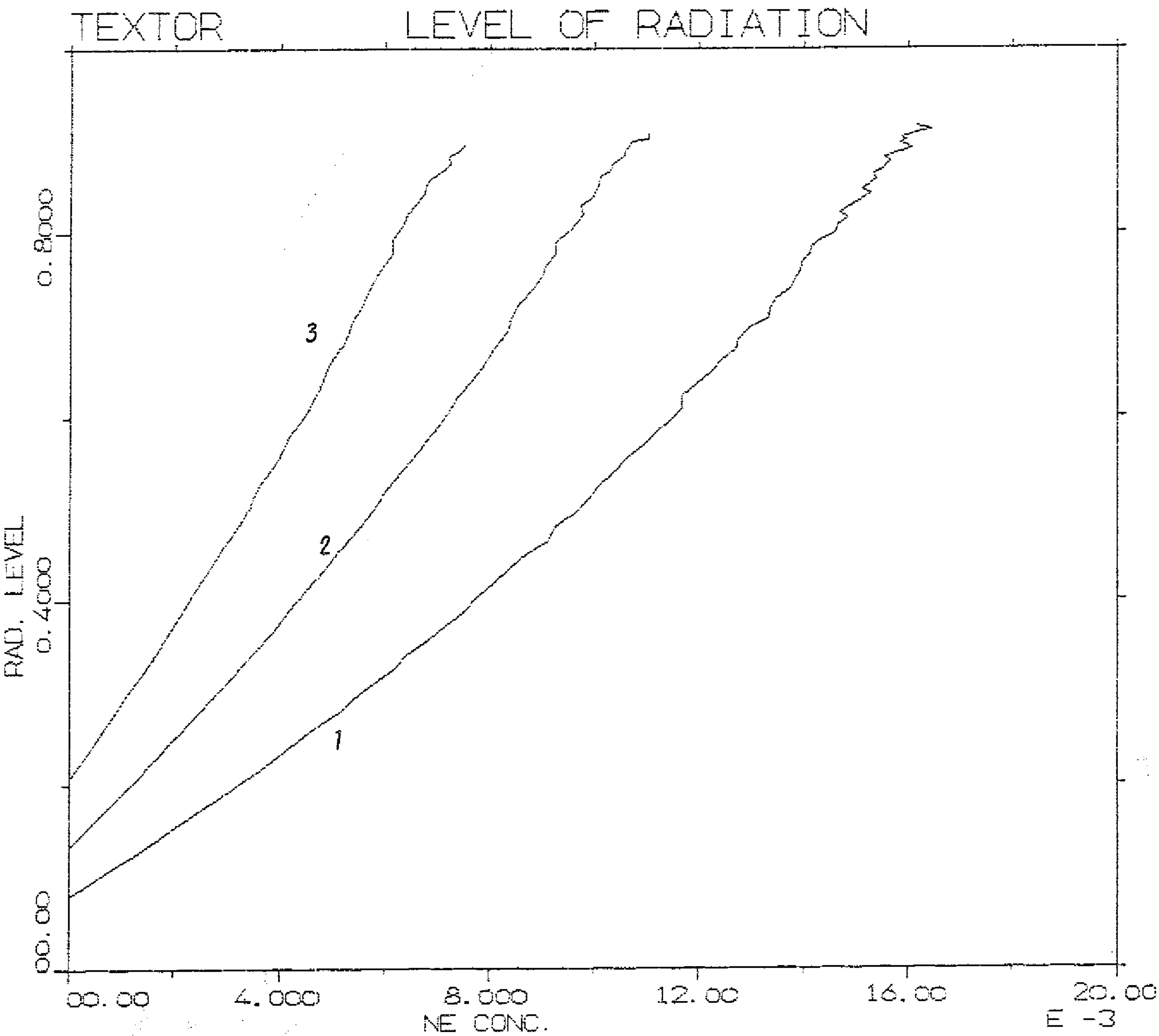

Fig.10 - Radiation level α_r in TEXTOR auxiliary heated discharges as a function of neon concentration c_{Ne}:
1 - $n_b = 4.4 \cdot 10^{13} cm^{-3}$, 2 - $n_b = 5 \cdot 10^{13} cm^{-3}$, 3 - $n_b = 5.6 \cdot 10^{13} cm^{-3}$.

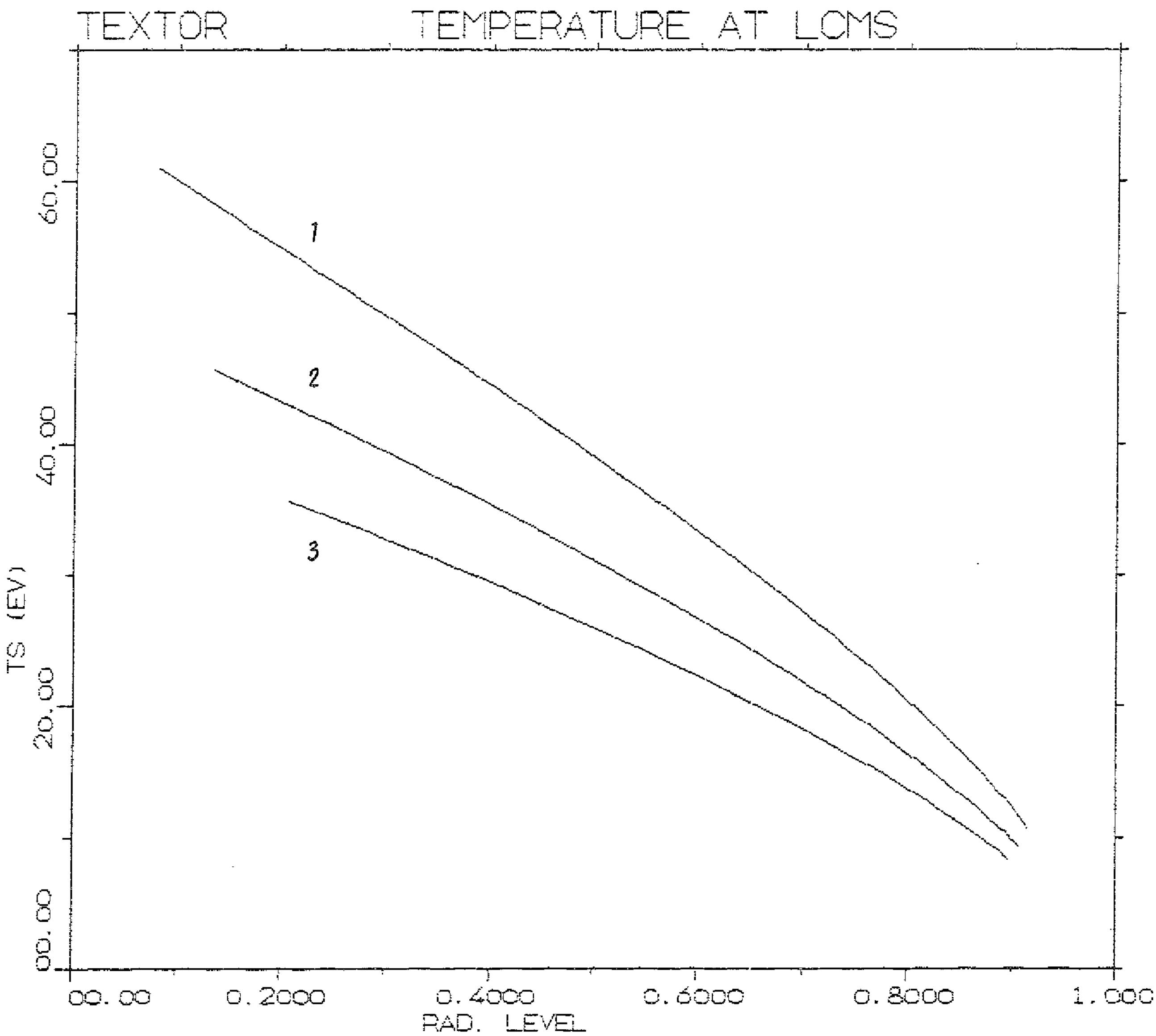

Fig. 11 - Dependence of the plasma temperature at the LCMS on the radiation level:
1 - $n_b = 4.4 \cdot 10^{13} cm^{-3}$, 2 - $n_b = 5 \cdot 10^{13} cm^{-3}$, 3 - $n_b = 5.6 \cdot 10^{13} cm^{-3}$.

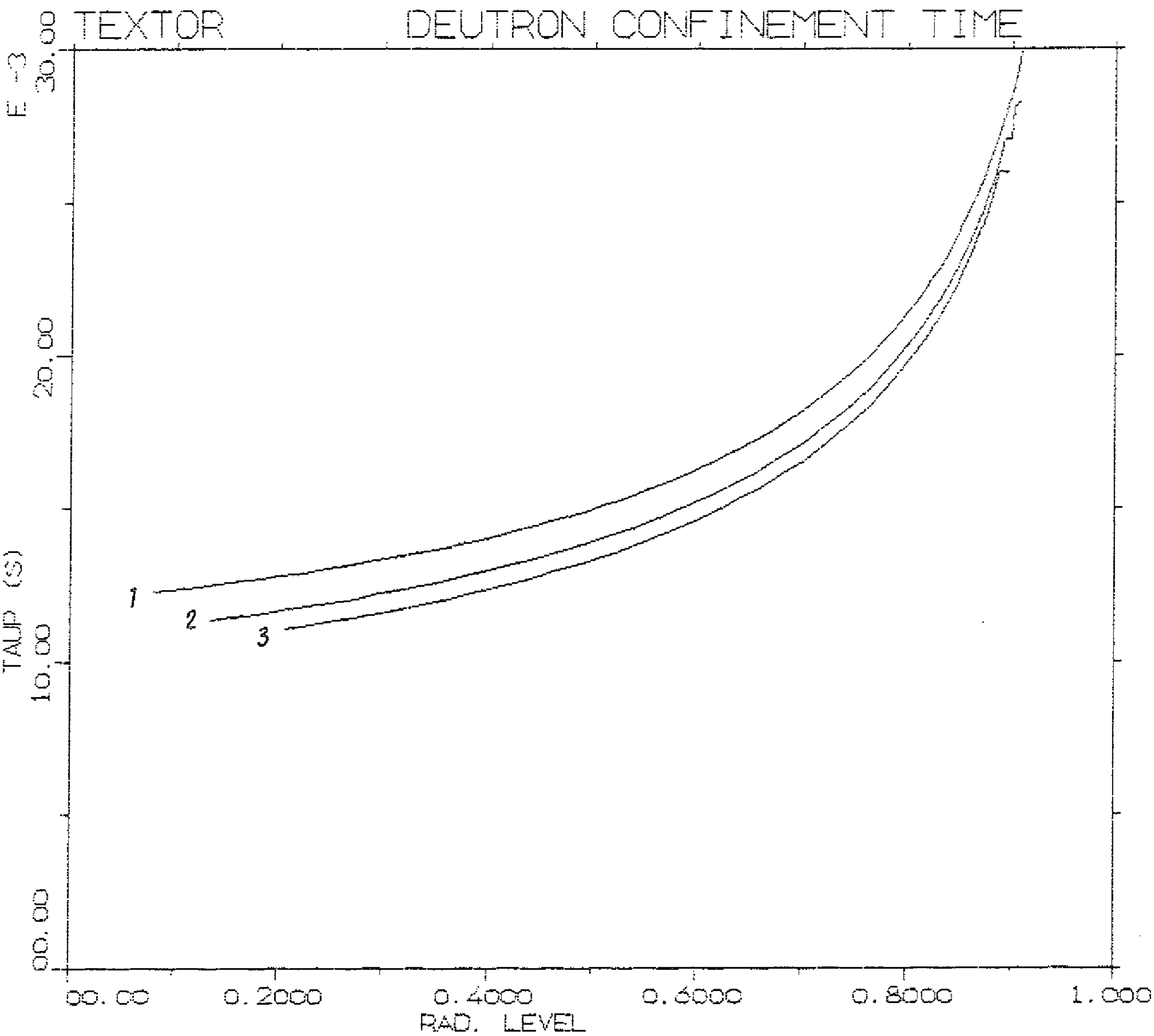

Fig. 12 - Dependences of the particle confinement time on the radiation level: 1 - $n_b = 4.4\cdot10^{13}cm^{-3}$, 2 - $n_b = 5\cdot10^{13}cm^{-3}$, 3 - $n_b = 5.6\cdot10^{13}cm^{-3}$.

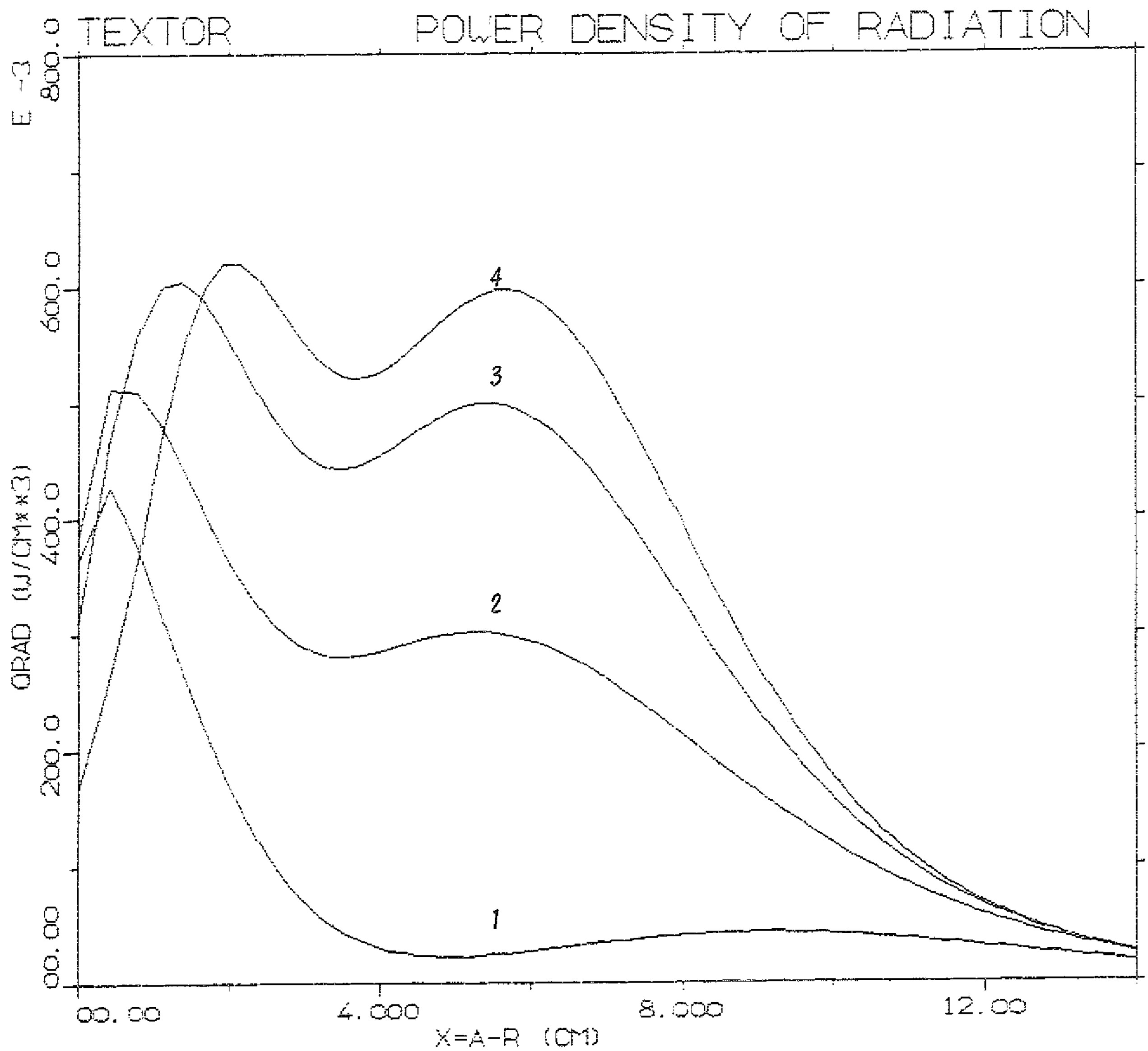

Fig.13 - Calculated profiles of the power density of the impurity radiation (n_b = $5.6 \cdot 10^{13} cm^{-3}$):
1 - α_r =0.16, 2 - α_r =0.34, 3 - α_r =0.67, 4 - α_r =0.91.

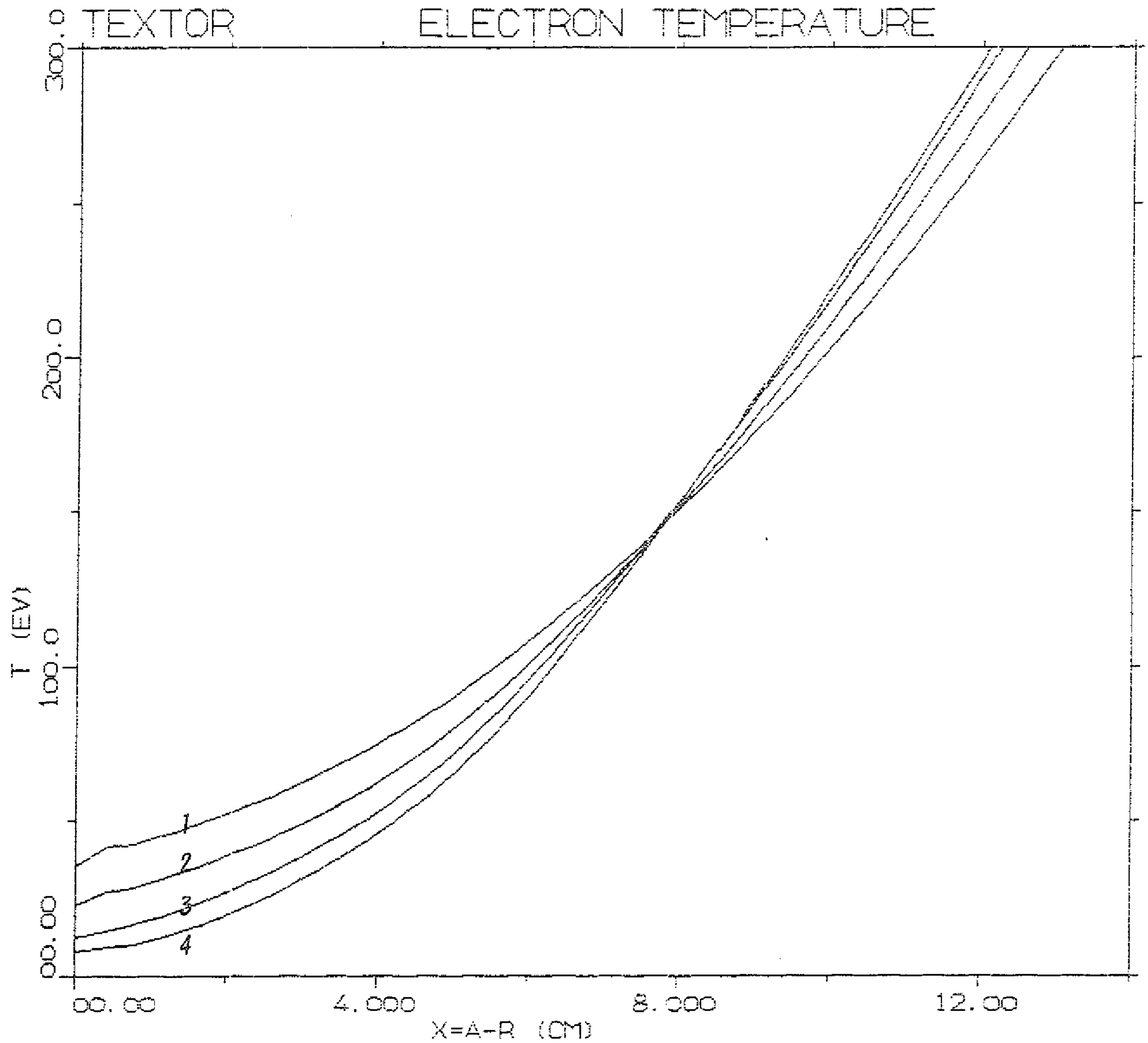

Fig.14 - Calculated profiles of the plasma temperature ($n_b = 5.6 \cdot 10^{13} cm^{-3}$): 1 - $\alpha_r = 0.16$, 2 - $\alpha_r = 0.34$, 3 - $\alpha_r = 0.67$, 4 - $\alpha_r = 0.91$.

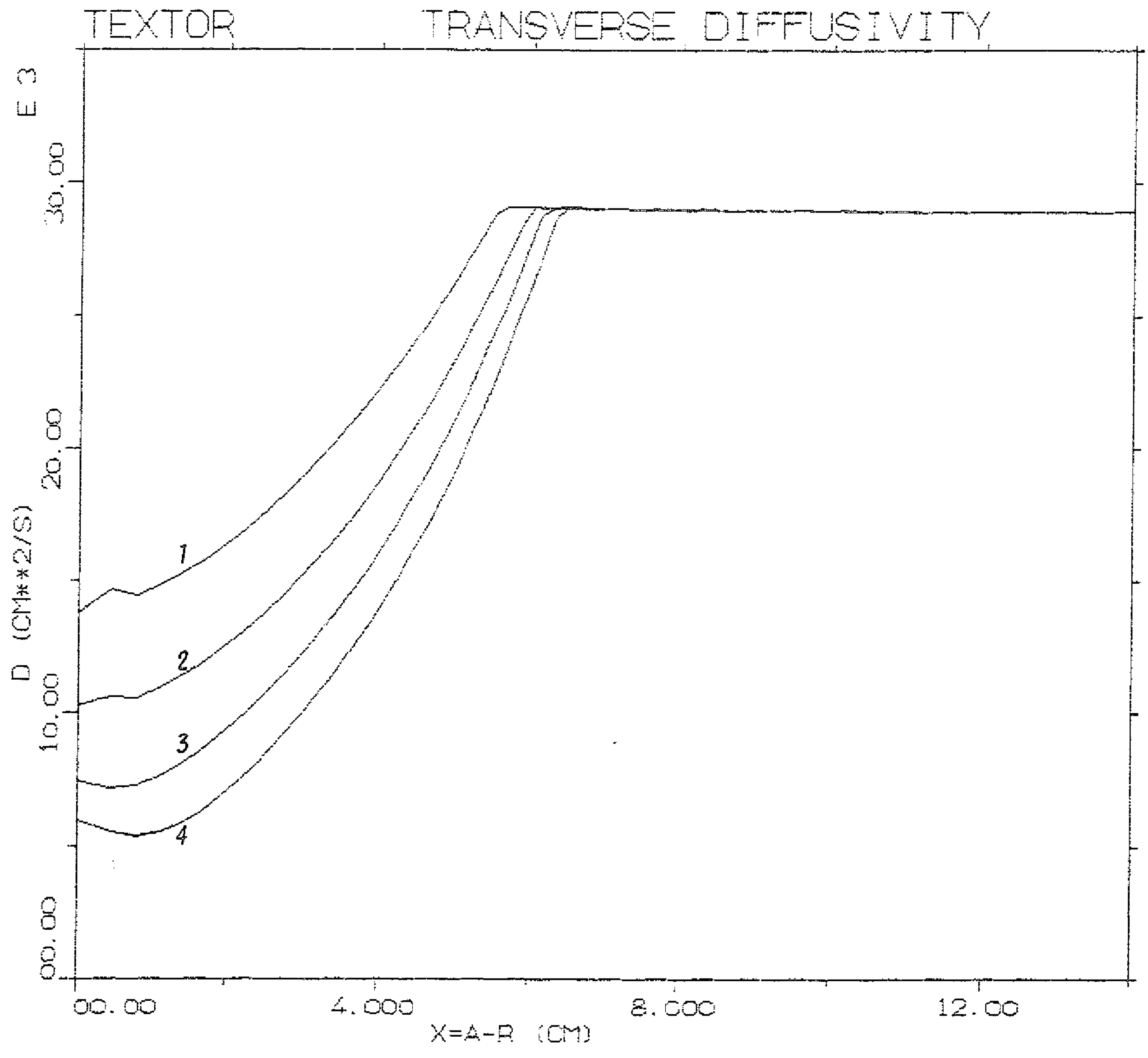

Fig.15 - Calculated profiles of the plasma diffusivity ($n_b = 5.6 \cdot 10^{13} cm^{-3}$): 1 - $\alpha_r = 0.16$, 2 - $\alpha_r = 0.34$, 3 - $\alpha_r = 0.67$, 4 - $\alpha_r = 0.91$.

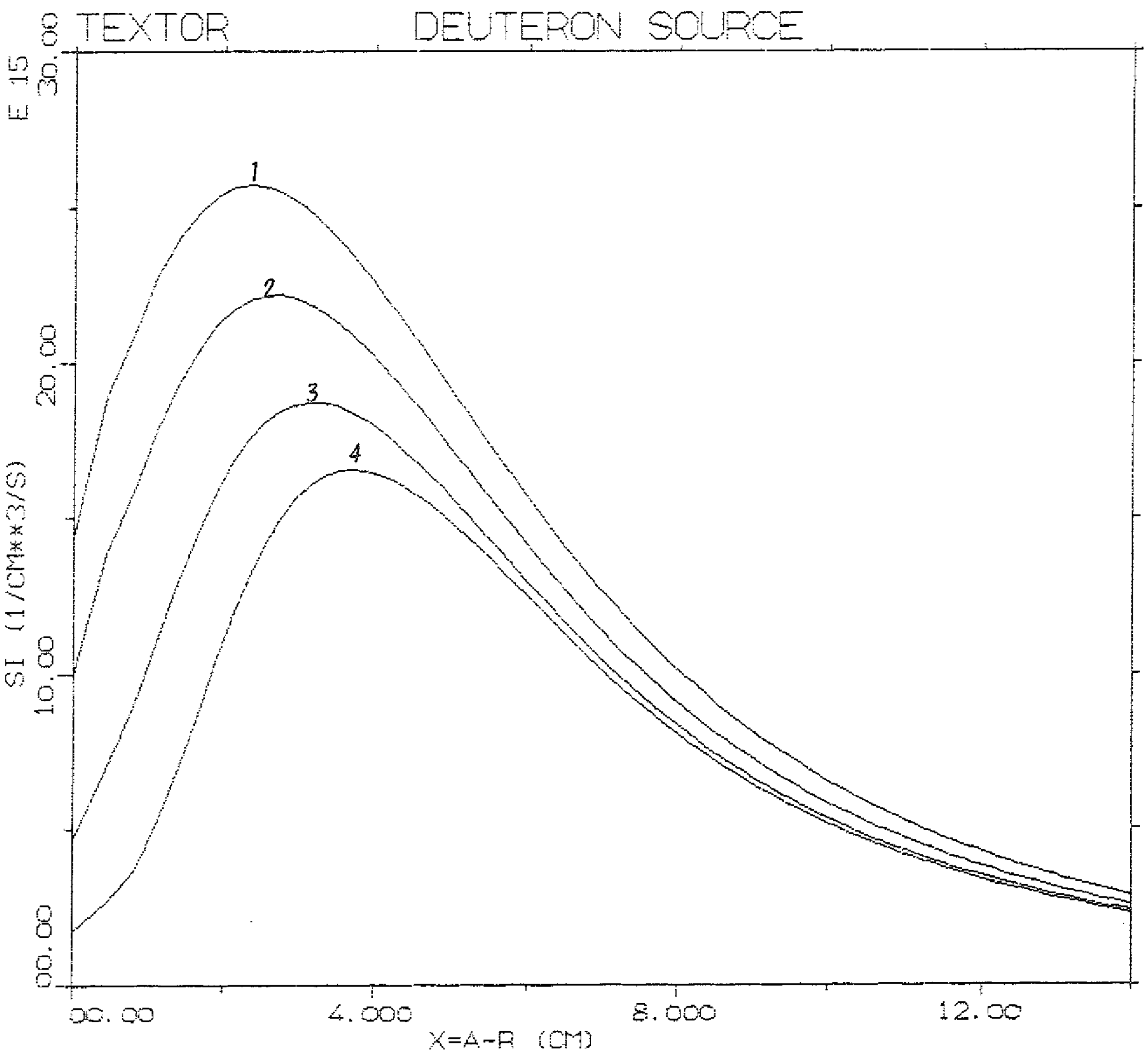

Fig.16 - Calculated profile of the deuteron source ($n_b = 5.6\cdot10^{13}cm^{-3}$):
1 - α_r =0.16, 2 - α_r =0.34, 3 - α_r =0.67, 4 - α_r =0.91.

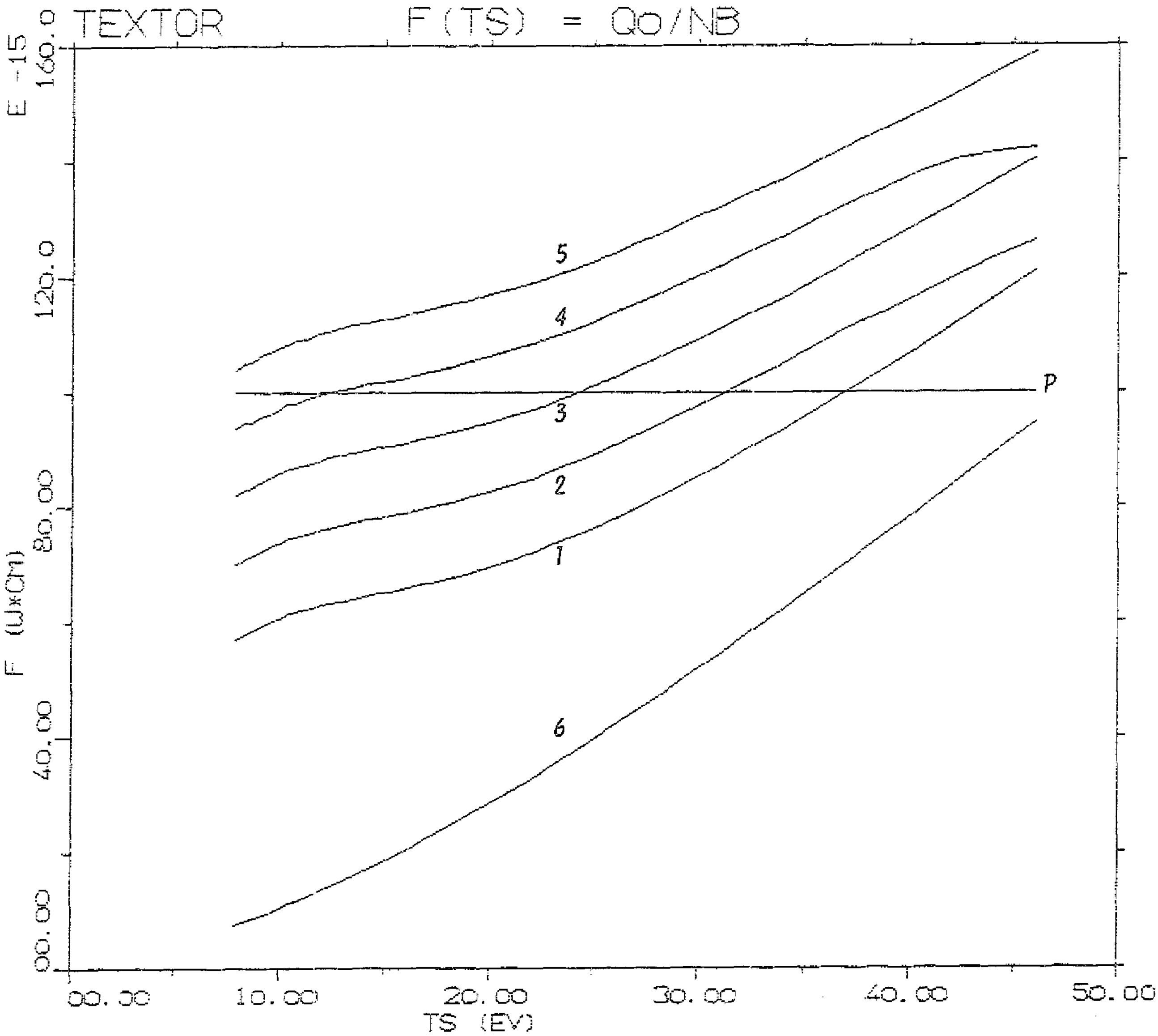

Fig.17 - Function $F(T_s)$ with $n_b = 5.6 \cdot 10^{13} cm^{-3}$:
1 - c_{Ne} = 0.18%, 2 - c_{Ne} = 0.36%, 3 - c_{Ne} = 0.54%, 4 - c_{Ne} = 0.72%,
5 - c_{Ne} = 0.9%,
6 - the part of F, corresponding to the heat losses in the SOL with particles.

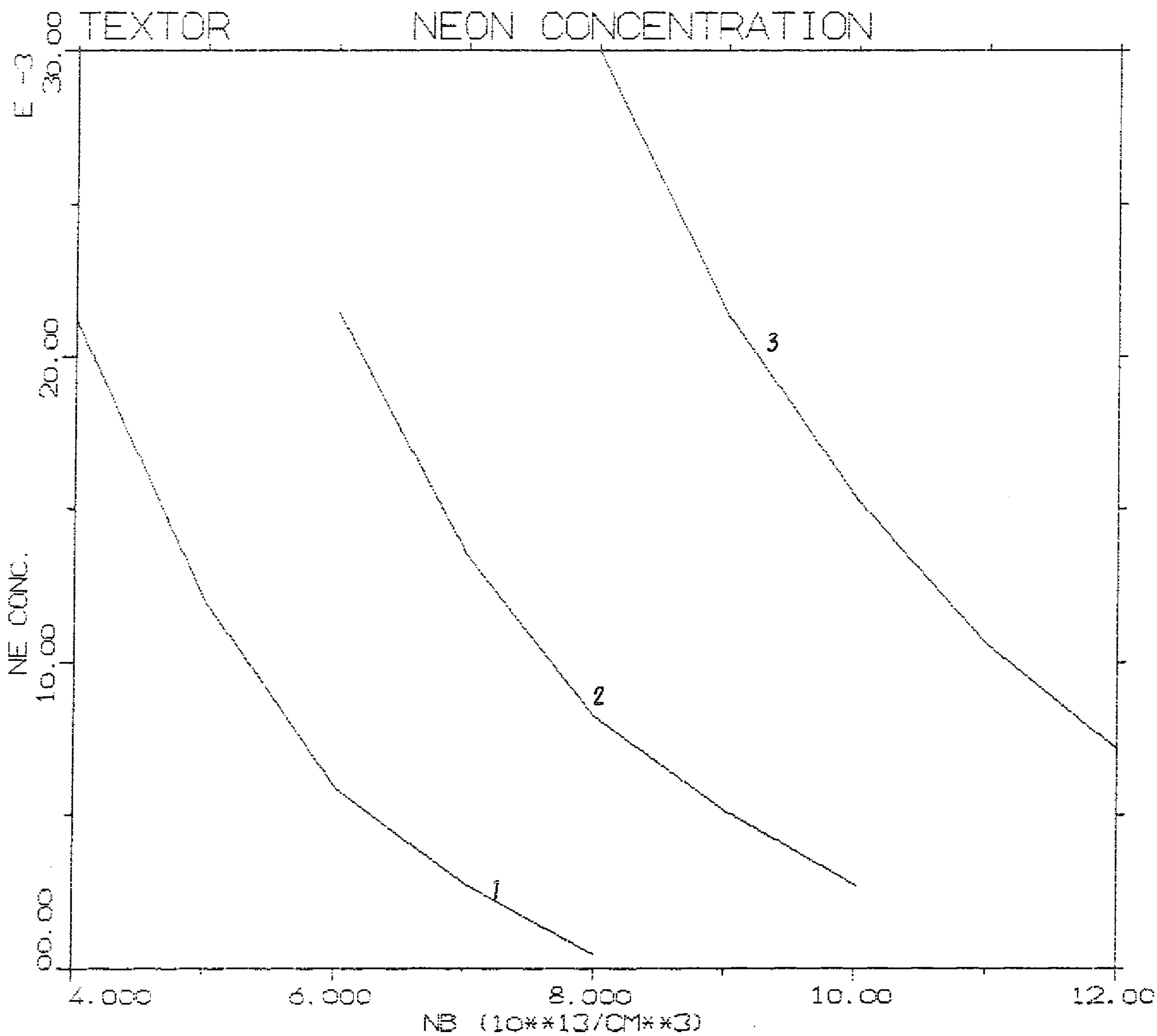

Fig. 18 - Dependence of the neon concentration needed for radiation of 90% of the power on the boundary plasma density n_b:
1 - q_0 = 5.5 W/cm^2, 2 - q_0 = 11 W/cm^2, 3 - q_0 = 22 W/cm^2.

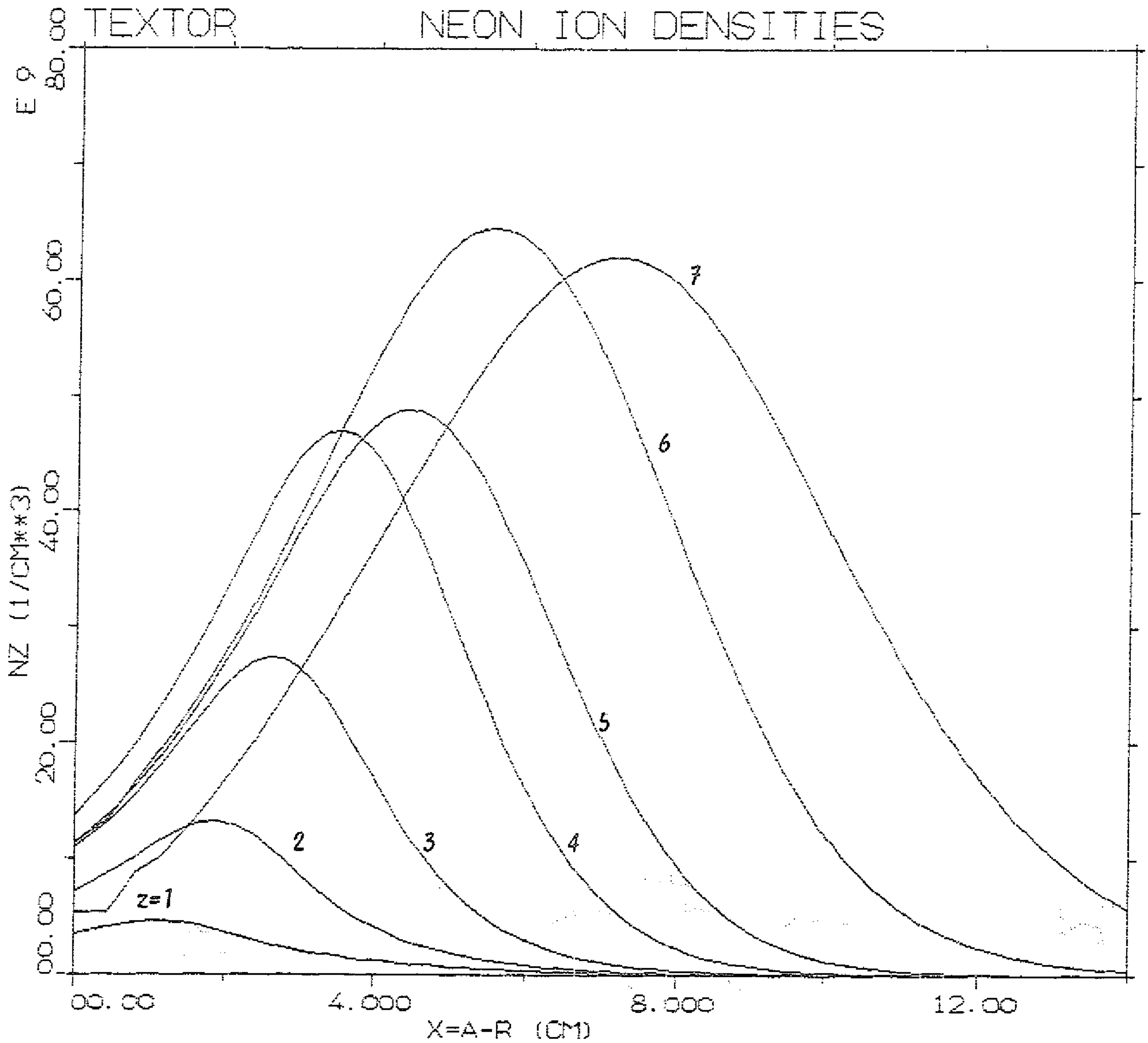

Fig.19 - Calculated profiles of the neon ion densities with $n_b = 5.6 \cdot 10^{13} cm^{-3}$ and $\alpha_r = 0.88$.

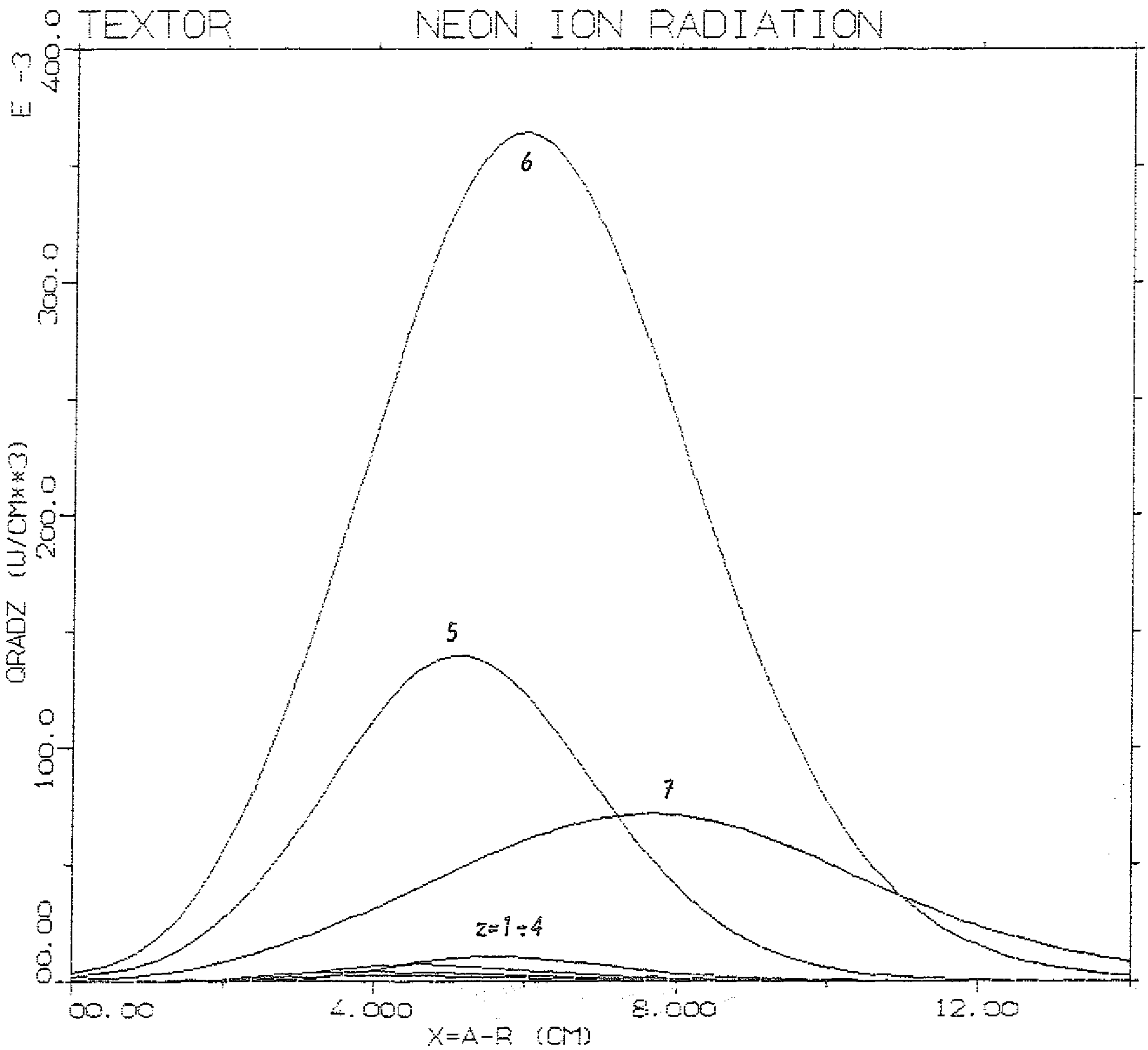

Fig.20 - Calculated profiles of the power densities of the neon ion radiation with $n_b = 5.6 \cdot 10^{13} cm^{-3}$ and $\alpha_r = 0.88$.

FORSCHUNGSZENTRUM JÜLICH GmbH

KFA

Jül-2588
February 1992
ISSN 0366-0885